NeuroImage 240 (2021) 118379

Contents lists available at ScienceDirect

NeuroImage

journal homepage: www.elsevier.com/locate/neuroimage

Structural and resting state functional connectivity beyond the cortex

Olivia K. Harrison[a,b,c,*], Xavier Guell[d,e,1], Miriam C. Klein-Flügge[f,1], Robert L. Barry[g,h,i,1]

[a] School of Pharmacy, University of Otago, New Zealand
[b] Translational Neuromodeling Unit, Institute for Biomedical Engineering, University of Zurich and ETH Zurich, Switzerland
[c] Nuffield Department of Clinical Neurosciences, University of Oxford, United Kingdom
[d] Massachusetts General Hospital, Harvard Medical School, United States
[e] Massachusetts Institute of Technology, United States
[f] Wellcome Centre for Integrative Neuroimaging, Department of Experimental Psychology, University of Oxford, United Kingdom
[g] Athinoula A. Martinos Center for Biomedical Imaging, Department of Radiology, Massachusetts General Hospital, United States
[h] Department of Radiology, Harvard Medical School, United States
[i] Harvard–Massachusetts Institute of Technology Health Sciences & Technology, United States

ARTICLE INFO

Connectivity
Amygdala
Brainstem
Cerebellum
Spinal cord

ABSTRACT

Mapping the structural and functional connectivity of the central nervous system has become a key area within neuroimaging research. While detailed network structures across the entire brain have been probed using animal models, non-invasive neuroimaging in humans has thus far been dominated by cortical investigations. Beyond the cortex, subcortical nuclei have traditionally been less accessible due to their smaller size and greater distance from radio frequency coils. However, major neuroimaging developments now provide improved signal and the resolution required to study these structures. Here, we present an overview of the connectivity between the amygdala, brainstem, cerebellum, spinal cord and the rest of the brain. While limitations to their imaging and analyses remain, we also provide some recommendations and considerations for mapping brain connectivity beyond the cortex.

1. Introduction

The advent of neuroimaging techniques has allowed us to move beyond animal models to examine the structure and function of networks within the human brain. However, brain connectivity research has thus far been dominated by investigations in cortical regions, with fewer studies focusing on the role of (often less accessible) subcortical structures. Herein we present a brief overview of brain connectivity beyond the cortex, with a specific focus on the amygdala, brainstem, cerebellum, and spinal cord. Each section covers the major neuroimaging developments that have advanced our knowledge regarding the structural and resting state functional connectivity of these respective non-cortical structures. While functional coupling within the brain is routinely measured using non-invasive techniques such as electroencephalography (EEG), magnetoencephalography (MEG) and functional near-infrared spectroscopy (fNIRS), these all suffer from poor sensitivity towards signals from deep within the brain. Hence, our discussion of resting state functional connectivity will be centered around functional magnetic resonance imaging (fMRI) as a method of choice for investigating these subcortical structures. We conclude with some recommendations for imaging and analysis practices that should be considered when analyzing connectivity beyond the cortex.

2. Forebrain subcortical regions: focusing on the amygdala as an example

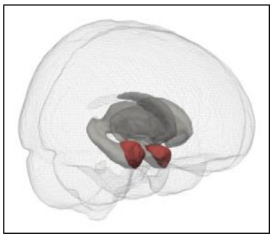

2.1. Overview

During brain development, forebrain subcortical structures develop from the embryonic prosencephalon, which divides into the diencephalon and telencephalon. The diencephalon consists of exclusively

* Corresponding author at: School of Pharmacy, University of Otago, New Zealand.
E-mail address: olivia.harrison@otago.ac.nz (O.K. Harrison).
[1] These authors contributed equally to this work.

https://doi.org/10.1016/j.neuroimage.2021.118379.
Received 8 February 2021; Received in revised form 21 May 2021; Accepted 7 July 2021
Available online 10 July 2021.

subcortical structures located on either side of the third ventricle: thalamus, epithalamus, subthalamus and hypothalamus. By contrast, the telencephalon develops into both cortical and subcortical regions. Subcortically, it comprises the amygdala, hippocampus, basal ganglia (putamen, caudate nucleus), globus pallidus, subthalamic nucleus, claustrum and basal forebrain.

Forebrain subcortical structures monitor and adjust, among other processes, sleep, homeostasis, alertness, emotion, motivation, endocrine responses and memory functions. Each subcortical region has a unique set of connections, yet the majority of neuroimaging work has focused on the connectivity between cortical regions (Biswal et al., 1995; Glasser et al., 2016; Horn et al., 2014; Mars et al., 2013; Neubert et al., 2014; Sallet et al., 2013). However, with advances in neuroimaging and suitable adjustments to standard methods, it is now possible to investigate the structural and functional connectivity of subcortical regions located deep inside the brain. In this first section, we will focus on the connectivity of the amygdala, a region that has been studied in-depth across mammalian species and which plays a central role in psychiatric disorders (Drevets, 2003; Murray et al., 2011). Some of the neuroimaging challenges and advances discussed in this section similarly apply to other forebrain subcortical structures. Covering the connectivity of all forebrain subcortical structures is outside the scope of this review.

The amygdala is located anterior to the hippocampus in the medial temporal lobe and is part of the limbic system. It is a phylogenetically old structure and critical for emotion regulation, fear conditioning and cognitive functions such as value-based decision-making (Adolphs, 2013; Aggleton, 1993; Chang et al., 2015; Grabenhorst et al., 2012; Klein-Flügge et al., 2019; Monte et al., 2015; Murray and Wise, 2010; Phelps and LeDoux, 2005). Several detailed atlases exist for subcortical regions more generally and the amygdala in particular (Ding et al., 2017; Keuken et al., 2014; Mai et al., 2015; Saygin et al., 2017; Tian et al., 2020). However, as is the case for all structures located deep within the brain, neuroimaging signals in the amygdala are hampered by its distance from the head coils (g-factor; (Pruessmann et al., 1999; Robson et al., 2008)). In addition, the medial temporal lobe is prone to distortions and signal loss induced by air/tissue boundaries, which cause non-uniformities in the magnetic field. Physiological artefacts arising from respiration and cardiac activity further distort the signal. Finally, the amygdala is not a homogenous structure, but a collection of multiple small dissociable – yet interconnected – nuclei, which further complicates the interpretation of signals recorded from this area.

Recent improvements in neuroimaging approaches for subcortical structures such as the amygdala include parallel imaging with multi-channel head-coils, reduced and/or multiple echo times, reversing of the phase-encoding direction to control for the direction of distortions, and smaller voxel resolution and slice thickness achieved through higher magnetic field strengths (Barch et al., 2013; Kundu et al., 2017; Robinson et al., 2004; Smith et al., 2013; Uğurbil et al., 2013). These measures help to overcome some of the challenges in acquiring data from subcortical structures highlighted above: they help reduce drop-out, and the improved resolution reduces partial volume effects and allows distinguishing different amygdala nuclei. In the amygdala in particular, however, care should be taken not to confound fMRI signals with activation in nearby veins (Boubela et al., 2015). In general, the trade-off between voxel size and signal-to-noise ratio (SNR) remains: Whilst smaller voxels have a penalty in terms of SNR, the resulting images may suffer less from partial volume effects (where a strong signal in part of a large voxel is less detectable than if it filled a small voxel) and from signal dropout (where local distortions in the magnetic field cause total loss of signal in a large voxel, but less across a small voxel).

2.2. Structural connectivity

The majority of studies investigating the structural connectivity of the amygdala and other forebrain subcortical structures have relied on invasive experimental methods in animal models. Early descriptive accounts from the late 19th and early 20th century (e.g. Edinger 1896 and Johnston 1923) laid out a framework for the morphology and evolution of the amygdala and advocated to study its fiber systems. This was first implemented using lesion and axon degeneration studies (e.g. Fox 1943) and gained precision with the advent of anterograde and retrograde tracer methods in the late 1960s and 1970s (Cowan et al., 1972; Kristensson and Olsson, 1971).

Tracer studies showed that the amygdala exhibits direct pathways to various midbrain and lower brainstem nuclei including the reticular formation and periaqueductal gray (PAG). These pathways originate predominantly from the central nucleus of the amygdala (Aggleton, 2000,1980; Hopkins, 1975; Hopkins and Holstege, 1978; Krettek and Price, 1978; Price, 2003; Price and Amaral, 1981). The amygdala also projects to the hypothalamus and again, these fibers most strongly originate from the central nucleus (Hopkins and Holstege, 1978; Price, 2003), which is the amygdala's main nucleus for modulating autonomic and endocrine responses. Other major forebrain subcortical connections of the amygdala are with the ventral striatum (nucleus accumbens and ventral putamen), the basal forebrain including the bed nucleus of the stria terminals (BNST), the thalamus, and the hippocampus (Aggleton, 2000, 1980; Cho et al., 2013; Friedman et al., 2002; Fudge et al., 2002; Krettek and Price, 1978; Price and Amaral, 1981). Many of these are reciprocal connections, but the connection patterns vary between different amygdala nuclei (Fig. 1A).

Direct cortical connections of the amygdala are most pronounced with posterior agranular medial and orbital frontal cortex (MFC, OFC), anterior temporal regions (perirhinal, temporal pole, inferotemporal) and agranular insula (Aggleton et al., 1980; Amaral and Price, 1984; Carmichael and Price, 1995; Cho et al., 2013; Freedman et al., 2000; Ghashghaei et al., 2007). Amygdala connections become weaker in more anterior dysgranular and granular OFC and MFC regions (Aggleton et al., 2015; Amaral et al., 1992; Ghashghaei et al., 2007; Price and Drevets, 2010). Cortical connections are largely bidirectional. Inputs from sensory association cortices (vision, audition, somatosensation) most strongly project to the lateral nucleus of the amygdala, the main sensory input nucleus of the amygdala, while frontal cortical projections are most pronounced with the basal and auxiliary basal nucleus (Fig. 1A) (Aggleton, 2000; Carmichael and Price, 1995; Cho et al., 2013; Freedman et al., 2000; Stefanacci and Amaral, 2002).

Amygdala connections identified in animal models are preserved across mammalian species, including humans. Directly assessing amygdala connectivity *in vivo* in humans using non-invasive neuroimaging methods poses significant challenges as the white matter around the amygdala is not homogenous. The presence of major fibers of passage (e.g. internal capsule) and the cross-over of several fiber pathways (e.g. around the basal forebrain) means that diffusion tensor imaging (DTI) tractography can miss smaller fiber pathways such as the stria terminalis and amygdalofugal pathway using standard protocols. Furthermore, DTI cannot differentiate monosynaptic from polysynaptic connections.

Nevertheless, using strong priors from animal work and refined methodological approaches, the key amygdala tracts have now been reconstructed using diffusion-based methods and shown to follow the same architectural principles as in non-human primate species. By placing seeds in the core of the white matter bundles of interest and using the full probability distribution of the fiber directions, it was possible to accurately reconstruct amygdala-prefrontal connections including the amygdalofugal and uncinate pathways, and these were found to be preserved across humans and monkeys (Fig. 1C) (Folloni et al., 2019). The stria terminalis, the fiber pathway connecting the central amygdala to BNST, has been reconstructed using more constrained deterministic tractography approaches; the obtained tract also matched the same tract described in animal work and its microstructure was predictive of threat responses (Kamali et al., 2015; Koller et al., 2019; Oler et al., 2017). The uncinate and anterior commissure, both prominent white matter bundles connecting the amygdala with inferior frontal regions and with its counterpart in the other hemisphere, have also been traced using DTI

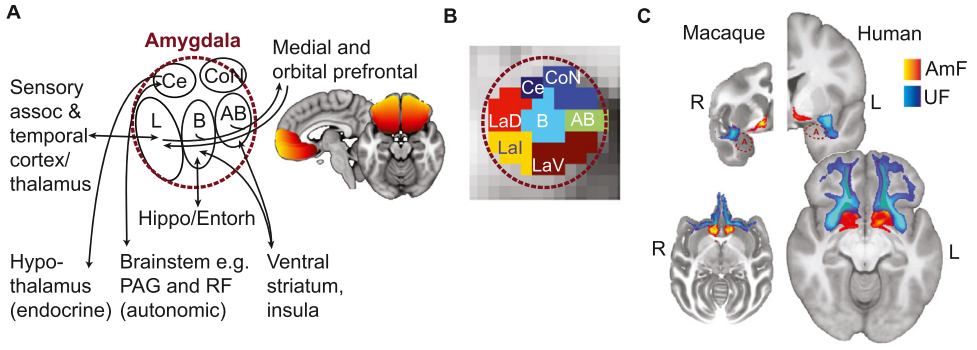

Fig. 1. A, Schematic summary of some of the major pathways to and from the amygdala discovered through invasive tracer techniques in animal models (adapted from Price (2003); Ce=central; CoN=cortical nuclei; L=lateral; B=basal; AB=auxiliary basal; PAG=periaqueductal gray; RF=reticular formation); in medial and orbital prefrontal cortex, there is a gradient (shown from red=strong to yellow=weak) with the strongest amygdala connections in posterior agranular regions and less dense projections to and from the amygdala in more anterior dysgranular and granular regions (Gashghaei and Barbas, 2007). **B**, Resting state neuroimaging data was used to parcellate the amygdala based on each voxel's connectivity pattern to the rest of the brain. This replicates the nuclei of the amygdala identified post-mortem at a fine spatial scale *in vivo* (LaD, LaI, LaV=dorsal, intermediate, and ventral divisions of lateral nucleus; adapted with permission from Klein-Flügge et al. (2019)), **C**, Probabilistic diffusion tractography can identify small tracts such as the amygdalofugal (AmF) and uncinate fasciculus (UF) (A=amygdala) and these are preserved across species (left=macaque; right=human; adapted with permission from Folloni et al. (2019), CC BY 4.0) (For interpretation of the references to color in this figure legend, the reader is referred to the web version of this article.).

tractography (Catani et al., 2002). Moreover, fiber density in a pathway between thalamus (pulvinar) and amygdala was shown to predict fear recognition (McFadyen et al., 2019).

DTI and tractography have also been used to identify subdivisions of the amygdala that differ in their connectivity profile. This has reliably identified two or three subdivisions such as the deep vs superficial nuclei, or the laterobasal, superficial and centromedial subdivisions (Bach et al., 2011; Balderston et al., 2015; Solano-Castiella et al., 2010).

2.3. Functional connectivity

Some of earliest work looking at functional coupling between the amygdala and other brain regions combined neural stimulation with direct recording techniques. This demonstrated, for example, that stimulating the basolateral amygdala elicited responses in the hypothalamus (Gloor, 1955). In humans, the functional coupling between two regions is typically measured non-invasively using functional magnetic resonance imaging (fMRI). Here, the temporal correlation between the blood oxygenation level dependent (BOLD) signal fluctuations of two regions (either at rest or during a task) is used as a measure of their functional connectivity. Resting state functional connectivity is a good proxy for anatomical connectivity (O'Reilly et al., 2013), and unlike diffusion tractography, it is not affected by crossing fibers or spatial distance. However, just like diffusion-based methods, it does not allow distinguishing mono-synaptic from poly-synaptic connections, nor is there inherently greater interpretability from the temporal correlations assessed in resting state analyses.

Hundreds of studies have investigated resting state functional connectivity in circuits involving the amygdala. The majority have focused on changes associated with different diseases, but some have focused on the basic properties of the amygdala's functional network. This has revealed distinct functional networks for the laterobasal, centromedial and superficial subdivisions of the amygdala, broadly resembling the circuits described in animal work (Bickart et al., 2012; Gorka et al., 2018; Grayson et al., 2016; Klein-Flügge et al., 2020; Oler et al., 2012; Roy et al., 2009; Weis et al., 2019). In addition, work examining functional connectivity has helped detect co-fluctuations between polysynaptically connected regions that are not typically reported in tracer studies. This has highlighted, for example, strong negative coupling between amygdala and dorso-lateral prefrontal cortex (dlPFC) (Doñamayor et al., 2017; Klein-Flügge et al., 2020), a target region for neurostimulation in depression.

Differences in the whole brain pattern of functional resting state coupling between voxels in the amygdala have also been used to identify amygdala subdivisions. While earlier work focused on two or three subdivisions (Bielski et al., 2021; Bzdok et al., 2013; Kerestes et al., 2017; Tian et al., 2020), a recent study identified seven nuclei per hemisphere based on *in vivo* resting state connectivity in the Human Connectome Project (HCP; Fig. 1B) (Klein-Flügge et al., 2020), and these closely resemble nuclei identified post-mortem (Saygin et al., 2017). In terms of the larger network architecture, the amygdala has generally been thought to be related to the default mode network (DMN) because of its strong connections with ventro-medial PFC (vmPFC). However, it diffusely integrates with several large-scale networks (Kerestes et al., 2017), not just the DMN, and this depends on the precise nucleus considered.

By far, the largest proportion of studies investigating amygdala functional connectivity has focused on changes in functional coupling as a function of stress and psychiatric illness. Importantly, connectivity markers are reliable across repeat-sessions, supporting its suitability as a potential biomarker (Nord et al., 2019). The most frequently reported coupling change is between amygdala and vmPFC/subgenual anterior cingulate cortex (sgACC), but the direction of change has not been entirely consistent across studies. *Reduced* coupling in this pathway has been observed after watching emotional compared to neutral movies (Eryilmaz et al., 2011), as a function of adverse life experiences in childhood (Park et al., 2018), cortisol levels (Veer et al., 2012), social anxiety (Hahn et al., 2011), state anxiety (Kim et al., 2011), and major depression (Cheng et al., 2018; Veer et al., 2010; Workman et al., 2016). By contrast, other studies have found *increased* coupling in the same pathway following a stress induction (Veer et al., 2011), in PTSD (Brown et al., 2014), and in major depression (Bijsterbosch et al., 2018; Connolly et al., 2013). SgACC is a site for deep brain stimulation (DBS) in treatment-resistant depression (Holtzheimer et al., 2017; Mayberg et al., 2005), and DBS works particularly well when the connections to subcortical regions are targeted (Johansen-Berg et al., 2007). Another circuit that has frequently been identified to be changed is between the amygdala and insula. Here, functional coupling relates to anxiety (Baur et al., 2013; Bijsterbosch et al., 2014) and acute stress (van Marle et al., 2010). However, thus far the majority of studies examining the functional connectivity of the amygdala do not consider the fine spatial scale of amygdala subdivisions, do not adequately correct BOLD data for physiological noise, do not have sufficient sample sizes, and the psychiatric illnesses under study are defined based on clinical criteria rather than specific pathophysiological mechanisms. These are all important aspects that future work will need to consider and which might aid identifying relationships between amygdala brain networks and changes in behavior (Klein-Flügge et al., 2020).

3. Brainstem

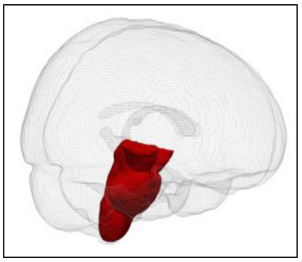

3.1. Overview

The brainstem is located deep and inferior within the brain, and comprised of three main areas: the midbrain, pons and medulla oblongata. Not only is the brainstem critical for the regulation of vital cardiac and respiratory functions, it is the main communication highway between the cortex/subcortex, cerebellum and spinal cord, and is intricately involved in the control of the central and peripheral nervous systems. Ten of the twelve pairs of cranial nerves either originate from or target brainstem nuclei, and the brainstem contains components of multiple motor and sensory systems such as the circuitry required for autonomic reflexes and the somatic nervous system. Furthermore, the reticular formation within the brainstem also contains nuclei associated with key modulatory and neurotransmitter systems, such as those involved in arousal, sleep and attention (cholinergic, serotonergic, noradrenergic and dopaminergic systems; see (Steward 2000) for a full overview and a description of the specific nuclei involved).

While some major brainstem structures have been visible *in vivo* using fMRI even at 0.35 tesla (Flannigan et al., 1985), accurately imaging the brainstem presents many significant neuroimaging challenges (Sclocco et al., 2018). These include (but are not limited to): an inherent reduction in SNR due to its depth and distance from the head coils; small nuclei with often poor image contrast; a large number of prominent surrounding white matter tracts; significant signal dropout in some susceptible MR images (such as those with T2* weighting) due to the often closely positioned facial sinuses, particularly in the pons region; and substantial artefacts in functional imaging induced by physiological noise from sources such as pulsatile vessels, respiratory-related movement, and bulk-susceptibility changes due to the close proximity of the brainstem to the lungs (Beissner, 2015; Brooks et al., 2013; Sclocco et al., 2018). As many of these challenges (with a particular emphasis on the influence of physiological noise) apply to all subcortical structures discussed in this review, we refer the reader to the "Issues and best practice" section for a summary and recommendations regarding the techniques available to minimize these effects.

To overcome the difficulty of anatomical discrimination of brainstem structures in early MRI, *ex vivo* histological slices were used for localization purposes (Flannigan et al., 1985). While the advent of high field 3 tesla imaging and head coil developments improved brainstem signal, the trade-off between improving spatial resolution and reducing SNR with decreasing voxel size remained prominent. However, the production of brainstem atlases such as those by Duvernoy (Naidich et al., 2009) and Paxinos (Paxinos and Huang, 2013) provided improved brainstem references, with unprecedented detail from both histological and post-mortem MR images. These atlases have been used in conjunction with techniques such as quantitative MRI and different scanning sequences that enable improved delineation of subcortical brainstem structures (e.g. quantitative MR and/or T2-weighted scans (Dunckley et al., 2005)). Finally, the use of both multi-slice imaging and ultra-high field (UHF) MRI at 7 tesla has now allowed drastic improvements in spatial resolution while maintaining required SNR, and the implications of this for brainstem imaging have been reviewed in detail elsewhere (Sclocco et al., 2018).

3.2. Structural connectivity

Animal models have permitted detailed neuronal mapping of the major descending motor and ascending somatosensory pathways through the brainstem. These include the descending pyramidal tracts (corticospinal and corticobulbar, originating in the cortex for voluntary motor control) and extrapyramidal tracts (vestibulospinal, reticulospinal, rubrospinal and tectospinal, originating in the brainstem for involuntary motor control), as well as the ascending somatosensory tracts (dorsal column medial lemniscal and the anteriolateral pathways, carrying sensory information for conscious perception) and spinocerebellar tracts (posterior spinocerebellar, cuneocerebellar, anterior spinocerebellar and rostral spinocerebellar, carrying sensory information for unconscious perception). Beyond passing fibers and relay stations, the brainstem also houses the nuclei and fascicles of 10 of the 12 cranial nerves, as well as countless other important nuclei, allowing for the control and integration of functions from numerous vital systems.

Despite the challenges of human brainstem imaging, large white matter pathways in the brainstem were mapped as early as 2001 using 1.5 T (Stieltjes et al., 2001). Here, brainstem DTI was undertaken *in vivo* to localize the major axonal pathways in the brainstem, including the corticospinal tract, medial lemniscus and cerebellar peduncles (Stieltjes et al., 2001). Following this work, *in vivo* atlases in stereotaxic space have been produced at 1.5 T (Mori et al., 2008, 2009), along with more recent and highly detailed *ex vivo* brainstem atlases (Aggarwal et al., 2013). These atlases allow us to visualize and quantify the structural connectivity both within the brainstem (Aggarwal et al., 2013) and between brainstem and cortex (Mori et al., 2008, 2009).

Beyond the measurement of white matter tracts that pass through and across the brainstem, structural connectivity analyses have also been undertaken to target and better understand key brainstem nuclei. The use of multi-contrast imaging (diffusion fractional anisotropy and T2-weighted) have aided the creation of probabilistic maps of key brainstem nuclei and systems, such as the ascending arousal, autonomic and motor systems (Bianciardi et al., 2015). Once specific anatomical targets have been identified, connectivity maps that utilize seed-based and hypothesis-driven approaches can be used to investigate brainstem nuclei and networks (Zhang et al., 2020) (Fig. 2). This technique has been used to consider the connectivity between the wider cortex and brainstem nuclei such as those within the ventral tegmental area and the cuneiform/subcuneiform nuclei and pedunculopontine nucleus (Englot et al., 2018). In clinical applications, a reduction in the ascending reticular activating system connectivity has been demonstrated in patients with epilepsy (Englot et al., 2018), and reductions in fractional anisotropy measurements in the dorsal and medial longitudinal fasciculi shown with increasing levels of chronic pain (Zhang et al., 2020). Furthermore, circuitry that encompasses both the brainstem and subcortex (such as the basal ganglia) has also been investigated in this manner using high-resolution *ex vivo* scanning (Plantinga et al., 2016). These targeted analyses allow us to answer specific questions about structural connectivity in the human brain and brainstem, and create comparisons to non-human models.

The structural connectivity profile between the brainstem and the rest of the brain has also been harnessed to aid even finer resolution and parcellate brainstem nuclei. For example, it was possible to delineate the subdivisions of the substantia nigra/ventral tegmental area (SN/VTA) based on their connectivity profiles to the striatum (Chowdhury et al., 2013), while the PAG subdivisions were elucidated by their connectivity to the rest of the brain (Ezra et al., 2015). In both instances, this technique generated parcellations that are anatomically plausible and consistent with animal models, and in the case of the SN/VTA, the subdivision connectivity pattern correlated with a reward-dependent personality trait (Chowdhury et al., 2013). This data-driven technique allows us to move beyond localization of anatomical structures within the brainstem, where (despite a lack of contrast) we can parcellate nu-

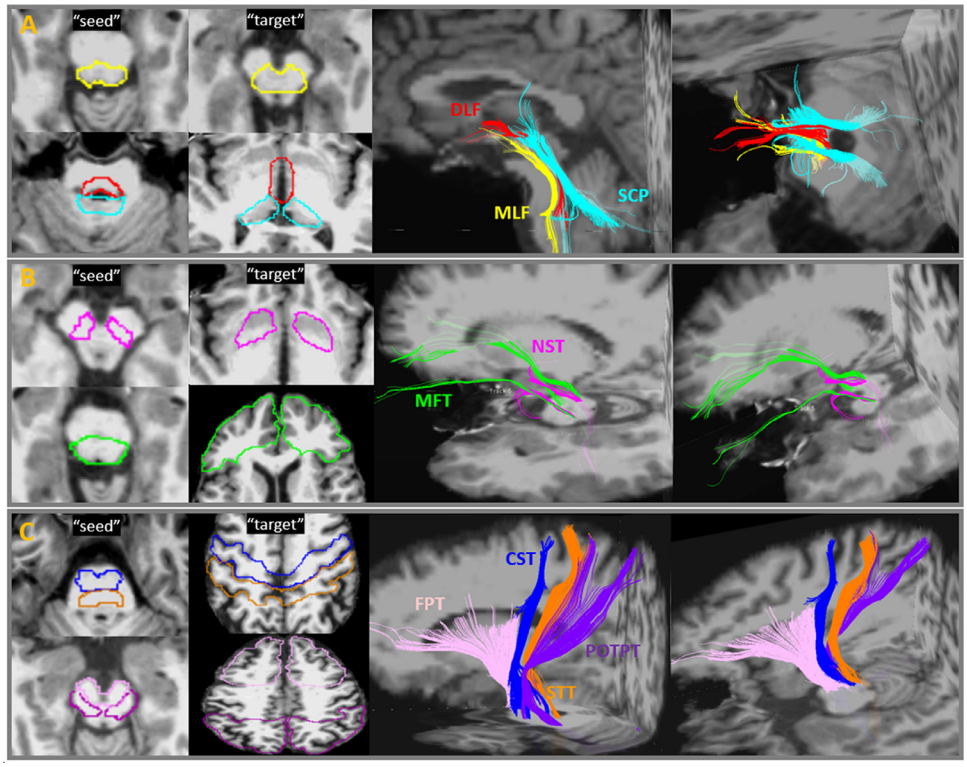

Fig. 2. Six brainstem fiber tracts (right) mapped using manual DTI, and the placement of the "Seed" and "Target" ROI-pairs (left) for each tract. Abbreviations: MLF=medial longitudinal fasciculus (yellow, A); DLF=dorsal longitudinal fasciculus (red, A); SCP=superior cerebellar peduncle (blue, A); MFT=medial forebrain tract (green, B); NST=nigrostriatal tract (magenta, B); FPT=frontopontine tract (pink, C); CST=corticospinal tract (blue, C); STT=spinothalamic tract (orange, C); POTPT=parieto-, occipito-, and temporopontine tract (purple, C). Figure from Zhang et al. (2020), reproduced under Creative Commons license (For interpretation of the references to color in this figure legend, the reader is referred to the web version of this article.).

clei based upon their structural connectivity profiles by leveraging rich brain-wide information.

3.3. Functional connectivity

Functional connectivity techniques have also been widely employed to investigate brainstem nuclei. As with structural connectivity, both seed-based and data-driven approaches have been utilized for brainstem functional connectivity analyses. When carefully performed, functional connectivity techniques can provide an alternative and nuanced understanding of the brainstem; the strong influence of the many passing white matter tracts no longer dominate as they do in structural connectivity analyses, and we may thus be more sensitive to the indirect connections between remote areas of the brain and the brainstem.

Seed-based functional connectivity analyses on resting state data have been used to map and compare connectivity profiles of the ascending brainstem arousal, autonomic and motor systems (Bianciardi et al., 2016). Additionally, targeted analyses of the monoamine-producing nuclei within the brainstem (Bär et al., 2016) have revealed connectivity differences resulting from the use of different antidepressants, employing drugs to target either noradrenergic and serotonergic neurotransmission or serotonergic neurotransmission only (Wagner et al., 2017). These results demonstrate the potential sensitivity of hypothesis-driven analyses within the brainstem. Finally, seed-based analyses at rest have also revealed differential functional connectivity between PAG subdivisions and the cortex, where seed location was determined by the functional activity during conditioned breathing tasks within the PAG (Faull and Pattinson, 2017). Using seeds derived from task-based analyses can lend themselves to more directed questions regarding functionally-active nuclei, as an alternative to anatomically-defined seeds. Beyond resting state, functional connectivity analyses that are performed *during* tasks (see Faull and Pattinson 2017, Sprenger et al. 2015 and Tinnermann et al. 2017 for specific examples of task-based functional connectivity of the PAG) can then assess how the brainstem may be functionally connected to the rest of the brain under specific conditions, or when performing certain functions. Further details regarding task-based functional connectivity are beyond the scope of this review.

Data-driven approaches have also been used to understand brainstem connectivity. Due to the reduced SNR and size of the brainstem in comparison to the cortex, standard techniques such as whole brain independent component analysis (ICA) are often dominated by cortical signal. To mitigate this effect, Beissner et al. (2014) proposed a two-stage technique of masked ICA within the brainstem, followed by backward regression of the identified components onto the wider cortex to identify their functional connectivity across the brain. This technique has revealed dissociable functional components within the brainstem that do not rely on anatomical localization procedures. The resulting cortical connectome maps were able to determine the relationship of these brainstem components to cortical structures, as well as identifying which components were likely driven by noise (via connectivity to cerebral spinal fluid compartments within the brain). These results demonstrate how functional connectivity techniques such as ICA can be applied to the brainstem, with special consideration taken for the challenges associated with brainstem and non-cortical analyses.

4. Cerebellum

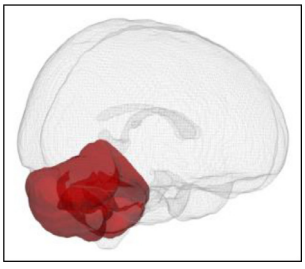

4.1. Overview

The cerebellum is located posterior to the pons and medulla separated by the fourth ventricle, and inferior to the cerebrum separated by the tentorium cerebelli. Despite its relatively small size, the cerebellum contains half of the total number of neurons in the brain. At a

gross anatomical level, the cerebellum is divided into two hemispheres, a midline structure named the vermis, and regions located immediately adjacent to the vermis named the paravermis (Felten et al., 2016). The interior of the cerebellum contains a mass of white matter and cerebellar nuclei, including the dentate, emboliform, globose, and fastigial nuclei. The exterior of the cerebellum, named the cerebellar cortex, is divided into three lobes and further subdivided into ten lobules. Lobules I-V form the anterior lobe, lobules VI-IX form the posterior lobe, and lobule X forms the flocculonodular lobe. Lobule VII is divided into VIIA and VIIB; Crus I and Crus II are subdivisions of lobule VIIA.

An extensive body of literature based on animal tract-tracing studies has defined the intricate pathways of connectivity between the cerebellum and the rest of the brain. Neuroimaging analyses in humans have replicated most major tracts of cerebellar structural connectivity, and further revealed that functional connections exist between the cerebellum and large-scale networks that involve all broad domains of human behavior.

4.2. Structural connectivity

Three cerebellar peduncles link the cerebellum to the spinal cord, brainstem, and cerebral hemispheres; these are the inferior, middle, and superior cerebellar peduncles (ICP, MCP, SCP). The cerebellar peduncles include many anatomical tracts; here we will highlight only a few notable connections. ICP includes afferent (input) fibers from the spinal cord that project to the cerebellar cortex. MCP carries afferent fibers into the cerebellar cortex from the pontine nuclei, which in turn receive afferents from the basal ganglia (Bostan et al., 2010) and the cerebral cortex. Connections between the cerebral cortex and the pons are of special interest, as they demonstrate the broad range of networks that are linked to the cerebellum. Sensorimotor cortical areas project to nuclei in the caudal pons (Brodal, 1979; Schmahmann et al., 2004). Beyond sensorimotor connections, there is also a wide spectrum of association areas in prefrontal, parietal, temporal, and cingulate cerebral cortical areas that target the rostral pontine nuclei (Schmahmann and Pandya, 1989, 1991, 1993, 1997). SCP carries output (efferent) fibers that link the cerebellum to the basal ganglia (Hoshi et al., 2005) and the thalamus. The thalamus then sends efferent projections to the cerebral cortex (Middleton and Strick, 1994). The dentate nuclei are especially relevant in these efferent connections, as they receive projections from all regions of the cerebellar cortex except from the vermis and paravermis, and serve as a relay station for these fibers before they reach the basal ganglia and thalamus via the SCP. In this way, the dentate nuclei connect the cerebellum to all major streams of information processing in the cerebral hemispheres. In contrast, the fastigial nuclei receive projections from the vermis and project mainly to vestibular and reticular nuclei, connecting cerebellar cortex to the reticulospinal and vestibulospinal tracts. Globose and emboliform nuclei receive projections from the paravermis and project mainly to the red nucleus, connecting cerebellar cortex to the rubrospinal tract.

Many connections of the cerebellum form closed-loop circuits. First, neurons in cerebellar nuclei project back to cerebellar cortical areas from which they receive input (Dietrichs, 1981). Second, each inferior olivary nucleus projects directly to a specific territory of cerebellar cortex, and includes afferent and efferent connections from the deep cerebellar nucleus that receives projections from the same territory of the cerebellar cortex (Zeeuw et al., 1998). Third, thalamic nuclei that are targeted predominantly by cerebellar cortical outputs will both send and receive projections to specific cerebral cortical areas (Guillery, 1995), which send projections to a pontine nucleus (Schmahmann and Pandya, 1997) that will then project back to the cerebellar cortical territory that is connected with that specific cerebral cortical area (Kelly and Strick, 2003).

Tract tracing investigations in rodents and primates are the basis of the overview of cerebellar connectivity provided above. Human neuroimaging studies of structural connections are inherently limited due to the dense packing of fibers in the cerebellar peduncles. This high degree of white matter density makes it challenging to determine the origin and destination of anatomical connections to and from the cerebellar cortex using MRI. Despite these limitations, human neuroimaging studies have provided a valuable opportunity to validate animal observations in the human brain, including connectivity analyzed between cerebellar cortex and cerebral cortex (Kamali et al., 2010; Karavasilis et al., 2019), cerebellar cortex and basal ganglia (Pelzer et al., 2013), or between sub-sections of these circuits such as between cerebellar cortex and deep nuclei, between deep nuclei and cerebral cortex, or between cerebellar peduncles and cerebral cortex (Granziera et al., 2009; Ji et al., 2019; Leitner et al., 2015; Steele et al., 2016; Takahashi et al., 2013; Toescu et al., 2020).

The fact that distinct parts of the cerebellar cortex are linked to distinct parts of the cerebral hemispheres has important implications for our understanding of cerebellar systems, computational and clinical neuroscience. These structural connections make it possible for distinct aspects of the cerebellar cortex to send and receive projections that belong to distinct motor, cognitive, and affective networks. Importantly, cerebellar cortical microstructure is essentially uniform (Ito, 1993; Voogd and Glickstein, 1998); while anatomical, physiological, and genetic regional differences exist between different regions of the cerebellar cortex (Cerminara et al., 2015; Zeeuw et al., 2020), these variations are minor compared to the degree of uniformity, and in sharp contrast with the notable variations in anatomy that are observed at a cellular level in the cerebral cortex (Guell et al., 2015, 2018a; Ramnani, 2006; Schmahmann, 1996, 2000, 2001, 2004; Schmahmann et al., 2007; Schmahmann and Pandya, 1991). These two contrasting anatomical realities – the heterogeneity in the targets of structural connections in the cerebellum, and the relative homogeneity of microstructural organization in the cerebellar cortex – indicates that there might be a similar neurological process that underlies the contribution of the cerebellum to multiple domains of behavior, and that there might be a similar direction of abnormality in the motor, cognitive, and affective symptoms that result from injury to the cerebellum (Universal Cerebellar Transform and Dysmetria of Thought theories) (Guell et al., 2015, 2018a; Schmahmann, 1996, 2001, 2004; Schmahmann et al., 2007; Schmahmann & Pandya, 1991). The specific nature of the Universal Cerebellar Transform as hypothesized in these studies is that the cerebellum performs its function by acting as an oscillation dampener, rapidly and automatically optimizing performance according to context. This singular neurological process emerges from an essentially uniform cerebellar cellular organization, and performs its computation on different channels of information processing subserved by anatomical connections that link focal cerebellar regions to different cerebral networks. The clinical consequence of this theory is that all motor, cognitive and affective symptoms that result from injury to the cerebellum are the manifestation of a disrupted Universal Cerebellar Transform, accounting for the similarities in the motor, cognitive, and emotional deficits that follow cerebellar injury.

Taken together, the structural connectivity of the cerebellum is highly complex, involves many neurological systems including extracerebellar territories of motor, cognitive and affective control, and is characterized by a high degree of reverberating (i.e., closed-loop) connections. The anatomical and functional connections that link the cerebellum to all major large-scale networks of the brain are the scientific basis of our modern understanding of the cerebellum as a modulator of movement, thought, and emotion – an organ that is relevant for disorders of motor control as well as for neurological and psychiatric diseases that degrade cognition and affect (Anteraper et al., 2019; Brady et al., 2019; D'Mello and Stoodley, 2015; Dong et al., 2020; Guell et al., 2020a,2020b; Guell et al., 2015, 2016; Hoche et al., 2016, 2018; Lee et al., 2020; Schmahmann and Sherman, 1998).

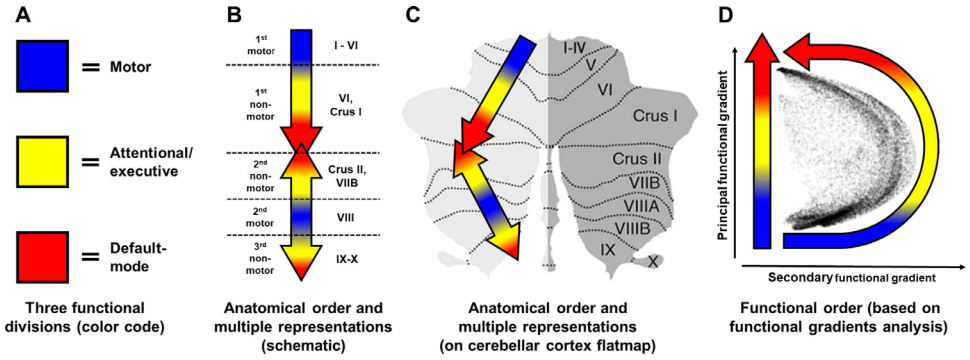

Fig. 3. *Summary of cerebellar functional organization based on human fMRI evidence.* (A) Three functional divisions of cerebellar cortex, based on Guell and Schmahmann et al. (2018). (B, C) Multiple representations of motor and non-motor function in the cerebellum and anatomical distribution of these representations, based on Buckner et al. (2011) and Guell et al. (2018b) (flat map of the cerebellum used as an anatomical Ref. Diedrichsen and Zotow (2015)). (D) The principal axis of macroscale functional organization in cerebellar cortex, including in functional connectivity from cerebellum to cerebellum and from cerebellum to cerebral cortex, progresses from motor, to attentional/executive, to default mode processing; a secondary gradient isolates attentional processing; based on Guell et al. (2018). All images in this figure are adapted from and further described in Guell and Schmahmann (2020).

4.3. Functional connectivity

Animal studies dominate the literature of structural connectivity in the cerebellum; neuroimaging analyses have served to confirm that cerebellar structural circuitry in the human brain is likely to follow similar general principles of organization as observed in the primate brain. In contrast, functional connectivity investigations have provided a completely novel dimension of knowledge that defines the complex relationships between brain and cerebellum, and situate the cerebellar cortex and cerebellar nuclei as central players in the organization of large-scale brain networks in all broad domains of human behavior (Buckner et al., 2011; Guell, Gabrieli, et al., 2018b, 2018; Habas et al., 2009).

Research using BOLD fMRI has shown that motor, attentional/executive (task-positive) and default mode (task-negative or inattentive) processing are the three fundamental poles of cerebellar cortical functional neuroanatomy (Fig. 3A). This principle holds true for analyses of intra-cerebellar functional connectivity, as well as for analyses of functional connectivity from cerebellar cortex to cerebral cortex (Guell et al., 2018). Motor, attentional/executive and default mode networks are organized anatomically in the cerebellar cortex obeying four principles, as follows (Guell and Schmahmann, 2020): (i) Motor function is represented twice in each cerebellar hemisphere, specifically in lobules I-VI and VIII. Non-motor function is represented three times, specifically in lobules VI-Crus I, Crus II-VIIB, and IX-X. In this way, there is a double motor and triple non-motor representation in the functional anatomy of the cerebellar cortex, including in its functional connectivity to the cerebral cortex (Buckner et al., 2011; Guell et al., 2018b) (Fig. 3B,C); (ii) A specific order from motor, to attentional/executive, to default mode territories is present throughout the cerebellar cortex; this order holds true for intra-cerebellar as well as for cerebellar-cerebral functional connectivity (Guell et al., 2018) (Fig. 3D); (iii) The first two principles result in the propagation of a specific ordering of functional connectivity (motor, attentional/executive, default mode) from first motor towards first non-motor representation (i.e., from lobules I-VI to Crus I), from second motor towards second non-motor representation (i.e., from lobule VIII to Crus II), and from second motor towards third non-motor representation (i.e., from lobule VIII to IX/X) (Fig. 3B,C); (iv) An anatomical peculiarity that results from these principles is that the intersection between Crus I and Crus II is the intersection of first default mode representation and second default mode representation. For this reason, first and second non-motor representations can be contiguous (as is the case for default mode processing) or separate (as is the case for attentional/executive processing) (Fig. 3B,C).

The evidence linking cerebellar functional connectivity to all major categories of neurological processing extends beyond the cerebellar cortex, and also includes the dentate nuclei (Bernard et al., 2014; Guell et al., 2019). Observing such a rich spectrum of functional diversity in the dentate nuclei is consistent with the anatomical reality that most territories of the cerebellar cortex project to them, and with the fact that cerebellar cortex contains representations of default mode, attentional, and motor connectivity. The same logic predicts a hypothesis that is yet untested – analogous brain compartments with connectivity to large portions of the human cerebellar cortex, such as pontine nuclei and inferior olivary nuclei, are likely possess a similar degree of functional diversity and complexity of organization.

5. Spinal cord

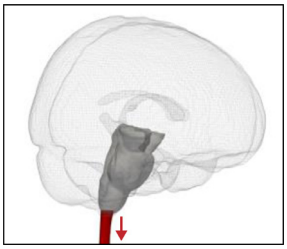

5.1. Overview

The spinal cord is a long, flexible structure that connects to the base of the brainstem and relays signals between the brain and body. It is the first point where sensory information is processed and is responsible for the conduction of electrical potentials involved in ascending sensory and pain stimuli and descending motor control between the brain and extremities. The spinal cord is composed of a butterfly-shaped densely packed gray matter column surrounded by white matter and meninges, and is suspended in a canal of cerebrospinal fluid and protected by a complex vertebral structure. Each side (left and right) of the gray matter column is divided into ventral (anterior) and dorsal (posterior) horns. The dorsal horn contains sensory neurons that receive information from the body's surface. Upper motor neurons synapse onto lower motor neurons in the ventral horn, which exit the spinal cord and innervate skeletal muscle (Kandel et al., 2000). A recent review details the rich complexity of spinal nerves and their projections throughout the peripheral nervous system (Irimia and Horn, 2021).

The three segments of the spinal cord are cervical, thoracic, and lumbar, although the thoracic and lumbar segments are often referred to contiguously as "thoracolumbar". Vertebral levels are clearly visible and map to spinal levels probabilistically (Cadotte et al., 2015; De Leener et al., 2017). Two defining features of the spinal cord are significant enlargements in cross-sectional area in the cervical cord at approximately C4/C5 and at the end of the thoracolumbar cord at T11/T12; at these locations, motor and sensory nerves innervating the arms and legs, respectively, make their synapses. The cross-sectional area of the cervical cord is ~50% larger than the thoracic

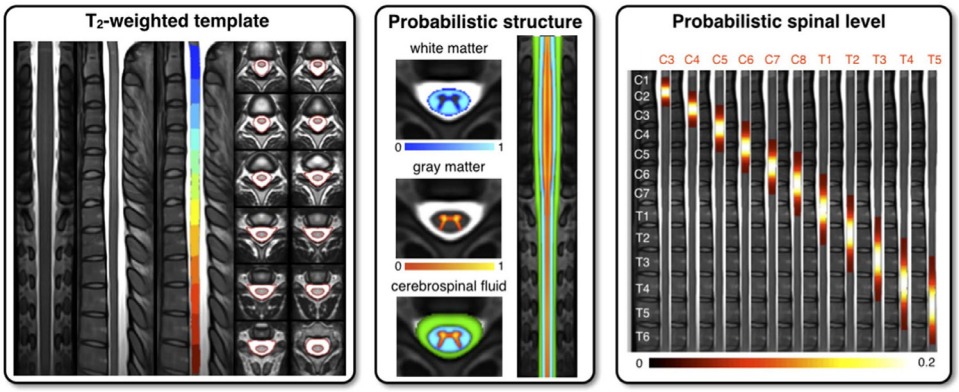

Fig. 4. *Template and atlases included in the Spinal Cord Toolbox*. (Left) Straight T2-weighted template with segmentation of vertebral levels, cerebrospinal fluid, and the spinal cord. (Middle) Probabilistic atlases of white and gray matter. (Right) Probabilistic map of spinal levels according to vertebral levels. (The white matter atlas is also included in the Toolbox but is not shown here.) Reproduced from De Leener et al. (2017) with permission from Elsevier.

cord (De Leener et al., 2018). At approximately L1/L2, the spinal cord quickly vanishes at the conus medullaris, and a bundle of nerves known as the cauda equina continues through the lumbar and sacral levels of the vertebral column.

The primary challenges of spinal cord fMRI are the small size of the spinal cord (~1 cm diameter) and gray matter regions of interest (~2-4 mm^2 in-plane, especially after eroding voxels along the gray/white matter boundary), reliable main field (B0) shimming, and high levels of physiological noise. The latter two challenges are additionally exacerbated at ultra-high fields (Barry et al., 2018). Unwanted signal variance attributable to physiological noise is particularly troublesome in the 'resting state' activity of the spinal cord as it is in close proximity to the throat, heart, lungs, and other internal organs. A secondary challenge was that, until recently, there was no "MNI-like" template or widely used open-source code for the spinal cord, thus making it almost impossible to compare or combine results across sites. The MNI-Poly-AMU and PAM50 templates (Fonov et al., 2014; De Leener et al., 2018) implemented within the Spinal Cord Toolbox (De Leener et al., 2017) now exist, thus forming a solid foundation upon which the field of resting state (and task-based) spinal cord fMRI may grow and thrive. Fig. 4 illustrates some of the templates and atlases available in the Spinal Cord Toolbox. Due to the disproportionate length of the cord relative to its cross-sectional diameter, the limited availability of MR scan time, and other considerations related to subject compliance and/or comfort, it is common for *in vivo* fMRI studies to image part of the cord (often the cervical region or a segment thereof) at high spatial resolution and use those results as an implicit proxy for the entire spinal cord. While MRI has played a role in spinal cord research for decades, the significant and unique challenges of imaging the cord compared to the cerebrum largely explain why developments in brain MRI have outpaced similar developments in spinal cord MRI. Nevertheless, recent advancements in MRI hardware and the development of the Spinal Cord Toolbox have mitigated some of the aforementioned challenges, thus fostering renewed interest in imaging and the recent surge of *de novo* spinal cord research.

5.2. Structural connectivity

The shape of the spinal cord reflects its evident structural connectivity along the rostral–caudal axis. Descending spinal cord tracts include ventral and lateral corticospinal, rubrospinal, tectospinal, vestibulospinal, ventral and lateral reticulospinal, and olivospinal. Ascending tracts include gracile fasciculus, cuneate fasciculus, ventral and dorsal spinocerebellar, ventral and lateral spinothalamic, spinoreticular, spinotectal, and spino-olivary. Descending pathways originating primarily in motor cortex are responsible for voluntary motor control. Projections along the lateral corticospinal tract decussate in the brainstem at the medulla oblongata while those in the ventral corticospinal tract decussate at the level of the corresponding segment in the cord. Corticospinal tract axons synapse onto neurons in ventral gray matter, from which efferent fibers exit the ventral roots of the cord and innervate specific muscle groups (Kandel et al., 2000; Purves et al., 2011). Mechanoreceptors and proprioceptors project onto the dorsal column medial lemniscus pathway (gracile and cuneate fasciculi) and encode information about fine touch, vibration, pressure, and position. A murine study has demonstrated the rich and complex modality segregation of ascending mechanoreceptors and proprioceptors in the dorsal white matter column (Niu et al., 2013). These receptors send first-order projections from ipsilateral dorsal root ganglia to the cord, where the axons travel along ipsilateral dorsal column tracts and synapse onto gray matter neurons in the medulla. For spinothalamic afferents, first-order axons from ipsilateral dorsal root ganglia enter the cord and synapse onto gray matter neurons in the ipsilateral dorsal horn (Kandel et al., 2000; Purves et al., 2011). The spinothalamic tract transmits fine touch, pain, and temperature, and spinothalamic fibers decussate at the level of the spinal cord and ascend contralaterally.

DTI investigations have not been as widespread in the spinal cord as in the brain, but studies have identified major white matter anatomies *in vivo* such as the corticospinal tracts, spinothalamic tracts, and dorsal column–medial lemniscus pathway (Ciccarelli et al., 2007). Within an axial slice, gray and white matter microstructures have been characterized using fractional anisotropy (FA), mean diffusivity, axial diffusivity, and radial diffusivity (By et al., 2016). Sequence optimizations have suggested no benefit in acquiring more than 15 diffusion gradient directions when measuring FA at 1.5T (Santarelli et al., 2010), and that measurement errors for these four diffusion metrics are minimal at 3T when 15 directions are used in a clinically feasible 9 min scan (By et al., 2016). A recent study investigated the impact of distortion corrections on spinal cord DTI (Dauleac et al., 2021). Another 3T study characterized the spinal cord's microstructure *in vivo* using the unique capabilities of the "Connectom" gradients (operating at 300 mT/m) and the Spinal Cord Toolbox's white matter atlas (De Leener et al., 2017): in spinal cord white matter, the average axon diameter was 4.5 ± 1.1 μm and ranged from 3.0 μm in the gracilis to 5.9 μm in the spinocerebellar tracts (Duval et al., 2015). High-resolution spinal cord DTI was also performed at an UHF of 7T with 0.8 × 0.8 × 3 mm^3 voxels (Massire et al., 2016, 2018) that was pushed to 0.4 × 0.4 × 10 mm^3 in one subject (Massire et al., 2018).

The potential clinical relevance for spinal cord DTI metrics has also been summarized in a recent review (Dauleac et al., 2021). For example, patients with multiple sclerosis exhibited lower connectivity and FA in the lateral corticospinal tracts and posterior tracts in C1–C3 compared to controls, suggesting that these metrics may be sensitive to disease-related tissue damage (Ciccarelli et al., 2007). In patients with amyotrophic lateral sclerosis, FA was lower in lateral and dorsal white matter columns in C2–T2, radial diffusivity was higher in lateral and dorsal white matter columns, and FA correlated with a composite clinical metric of functional impairment (ALSFRS-R) (Cohen-Adad et al., 2012). The aforementioned review (Dauleac et al., 2021) highlights the range

of acquisition parameters and analysis methods for spinal cord DTI and provides recommendations for improving diffusion data quality and interpretability. Finally, multi-modal investigations have also been conducted to validate microstructural measurements, thus bridging the gaps between clinical observations, *in vivo* DTI, and high-resolution histology and microscopy techniques (Cohen-Adad, 2018).

5.3. Functional connectivity

While resting state fMRI was first investigated in the brain a quarter-century ago (Biswal et al., 1995), similar investigations in the human spinal cord are much more recent but quickly growing in number. Compared to the enormous body of research examining resting or task-free conditions in the cerebral cortex, we have, as of December 2020 (when the initial draft of this manuscript was completed), identified 23 journal articles on resting state spinal cord fMRI (Barry et al., 2014, 2016; Barry et al., 2018; Chen et al., 2015; Conrad et al., 2018; Eippert et al., 2017; Harita et al., 2019; Harita and Stroman, 2017; Hu et al., 2018; Ioachim et al., 2019; Tinnermann et al., 2020; Kinany et al., 2020; Kong et al., 2014; Liu et al., 2016; Liu et al., 2016; Martucci et al., 2019; San Emeterio Nateras et al., 2015; Vahdat et al., 2020; Weber et al., 2018; Wei et al., 2009; Wu et al., 2018, 2019, 2020). These publications are briefly summarized in Supplementary Table S1. Of these articles, 19 report findings in humans, two in squirrel monkeys, and two in Sprague Dawley rats. Of the two non-human primate reports, the first characterized spinal cord connectivity before and after a unilateral injury at C5 (Chen et al., 2015), and the second performed multimodal spinal cord fMRI and electrophysiology (Wu et al., 2019). Of the two rodent studies, the first characterized the healthy spinal cord (Wu et al., 2018) and the second investigated the impact of a contusion injury (Wu et al., 2020). All non-human studies thus far have been performed at an ultra-high field of 9.4T.

In humans, the first attempt at resting state spinal cord fMRI reported a dominating signal associated with the expected frequency range of the respiratory cycle (Wei et al., 2009); as such, these results are equivocal and underscore the importance of properly mitigating sources of physiological noise in spinal cord fMRI (Eippert et al., 2017). The next study was performed at an UHF of 7T and reported robust temporal correlations between ventral horns and between dorsal horns within an axial slice, thus providing the first evidence of bilateral ventral (motor) and dorsal (sensory) resting state networks (Barry et al., 2014). A follow-up 7T study quantified the reproducibility of these networks within the same scanning session (Barry et al., 2016). The first 3T study using independent component analysis provided strong evidence for a ventral network (Kong et al., 2014); these data were re-analyzed with a seed-based approach and subsequently reported evidence for a dorsal network as well (Eippert et al., 2017). There is also evidence of ipsilateral ventral–dorsal (motor–sensory) connectivity in primates (Chen et al., 2015) and, to a lesser extent, humans (Weber et al., 2018); however, it is not yet clear if observed ventral–dorsal correlations are due to the close proximity of ipsilateral ventral and dorsal seed regions, or if they represent a tertiary network that might reflect quadrupedal vs. bipedal tendencies or possibly subserve reflexes. Connectivity between ipsilateral ventral and dorsal horns is certainly plausible and should continue to be investigated. Furthermore, some studies have considered the impact of methodological choices in the fMRI preprocessing pipeline (Barry et al., 2018; Barry et al., 2014; Eippert et al., 2017; Hu et al., 2018), thus contextualizing observed correlations as a function of preceding preprocessing steps and providing evidence on whether or not results may be artifactual due to suboptimal preprocessing decisions.

The first investigation of dynamic functional connectivity along the spinal cord has also been published (Kinany et al., 2020), opening the door to the application of more advanced neuroimaging techniques. Connectivity along the cord has been considered to characterize ascending sensory and descending motor pathways, and one group has employed a sagittal acquisition scheme to investigate networks and connectivity within and between the cervical cord and brainstem (Harita et al., 2019; Harita & Stroman, 2017; Ioachim et al., 2019, 2020). Connections have been reported between ventral/dorsal horns and the corticospinal tracts (Harita and Stroman, 2017), and while widespread connectivity between cervical levels has been reported (Ioachim et al., 2019), more evidence across species suggests that connectivity along the cord drops off significantly past one vertebral level (Chen et al., 2015; Harita et al., 2019; Kinany et al., 2020; Kong et al., 2014; Liu et al., 2016; San Emeterio Nateras et al., 2015; Weber et al., 2018; Wu et al., 2018, 2019).

It is, of course, crucial to translate new methods to clinical populations to investigate whether these functional methods are sensitive to spinal cord injury or disease. At 7T, functional connectivity was shown to be locally altered near visible lesions in patients with relapsing-remitting multiple sclerosis (Conrad et al., 2018). While most studies have investigated functional connectivity via seed regions and/or independent component analysis, two used the 'ALFF' (amplitude of low frequency fluctuation) (Zang et al., 2007) technique and reported differences in spinal cord ALFF between healthy controls and patients with cervical spondylotic myelopathy (Liu et al., 2016) or fibromyalgia (Martucci et al., 2019). Reports of differences in spinal cord connectivity before and after animal models of spinal cord injury (Chen et al., 2015; Wu et al., 2020) suggest that these techniques may also be applicable in characterizing spinal cord injury and functional recovery in humans.

In summary, while resting state spinal cord fMRI is a relatively young field, there is remarkable agreement in findings across human and non-human studies, field strengths, and acquisition, preprocessing and analysis methodologies. One question that has persisted, however, is whether spinal cord networks are separate and operate independently from resting state brain networks, or whether they manifest from the same processes that give rise to networks in the brain? While easy to pose, directly addressing this question has been challenging due to several factors including, but not limited to, an order of magnitude difference in size between these anatomies, disparate B0 shimming between the brain and cord, and a specialized protocol capable of acquiring functional images of the brain and cervical cord simultaneously (Finsterbusch et al., 2013; Tinnermann et al., 2020). Importantly, the first study to overcome these challenges and bridge this gap was recently published and provides compelling evidence in support of unified central nervous system resting state networks (Vahdat et al., 2020).

6. Issues and best practice

To help mitigate some of the challenges associated with non-cortical imaging and connectivity analyses, the following measures could be considered (see also Beissner 2015 and Sclocco et al. 2018):

- Piloting and comparing sequence options is critical to finding the compromise that best suits to answer the scientific question posed.
- Consider using MR techniques that will improve SNR, such as increased field strength, multi-slice and/or multi-echo imaging, and longer acquisition times (in some circumstances). However, be aware of the possible reduction in the relative SNR in the deep brain and brainstem that may be caused by techniques such as multiband acceleration, sensitivity to motion artefacts with multi-slice imaging (Vu et al., 2017), and potentially greater signal distortions with higher field strengths (Brooks et al., 2013; Vu et al., 2017).
- Choose a voxel resolution, slice thickness and echo time appropriate/optimal for the target nuclei or regions. Note that smaller voxel sizes need to be balanced against reductions at SNR and are therefore particularly appropriate at higher field strengths. Moreover, functional connectivity of regions or nuclei that contain several subdivisions (e.g. amygdala, see Fig. 1) can be difficult to interpret, especially for voxels at the boundary.
- For reducing drop-out and distortions, carefully consider choices such as the slice angulation which can have beneficial or detrimen-

tal effects on particular regions; also consider acquiring images with reverse phase-encoding directions to correct for distortions.

- Always measure and account for the effects of physiological noise using either prospective techniques such as sequence gating, or retrospective techniques such as RETROICOR (Glover et al., 2000) and independent component analysis (Griffanti et al., 2017; Kelly et al., 2010; Kundu et al., 2012; Thomas et al., 2002), possibly in association with noise classification algorithms such as ICA-FIX or ICA-AROMA (Pruim et al., 2015; Salimi-Khorshidi et al., 2014). The location of surrounding major vessels and pulsatile fluid-filled spaces, as well as the closer proximity to the lungs mean that non-cortical structures are more susceptible to the effects of physiological noise (Brooks et al., 2013). Furthermore, the effect of physiological noise can be particularly prominent in resting state fMRI, in the absence of task-based fluctuations in the BOLD signal.
- It may be appropriate to utilize scans with different contrasts (such as diffusion fractional anisotropy and T2-weighted images) to better visualize and differentiate the important nuclei that are being targeted, particularly such that accurate alignment and normalization can be performed.
- Use caution when applying spatial smoothing, considering the size of the structure being investigated. For example, cerebellar folia and subfolia are much smaller than cerebral cortical gyri; in contrast with flat maps of the cerebral cortex (Essen et al., 1998), flat maps of the cerebellum obtained within current limitations of most neuroimaging studies do not represent a true flat representation of all cerebellar cortical surface (Diedrichsen and Zotow, 2015). Additionally, masking and signal extraction of specific regions *prior* to smoothing may be beneficial, to avoid incorporating signals from structures such as ventricles, vessels, or neighboring nuclei into the data.
- Interpretation of non-cortical imaging findings based on anatomical boundaries may not always provide meaningful functional insights; for instance in the cerebellum, researchers should consider using available atlases based on functional connectivity (Buckner et al., 2011), task activation (King et al., 2019), or functional gradients (Guell et al., 2019; Guell, Schmahmann, et al., 2018).
- Functional localizers from task activity can be used to target and analyze the connectivity of subsections of nuclei that are active under specific conditions. However, the physiological meaning of fMRI signal is an ongoing topic of debate; since subcortical, brainstem, cerebellar and spinal cord cellular and vascular organization is different from the cerebral cortex, it is possible that fMRI signal in these areas cannot be interpreted in the exact same way (Logothetis and Wandell, 2004).
- Be aware that SNR is reduced subcortically compared to the cortex, and this will have implications for brain-wide models (such as ICA) that will likely be driven by more dominant cortical signal.
- Strong signals within the cortex can be harnessed as an advantage, such as using backward projection of diffusion tractography to either localize or parcellate subcortical regions.
- Finally, adjustments may need to be made in the statistical techniques employed when analyzing smaller subcortical structures; techniques such as cluster-wise inference may favor large clusters and reduce the ability to detect functional activity and/or connectivity within smaller nuclei.

Statement

No data or code was used in the production of this review manuscript. All Figures containing data have been reproduced from their original publications with the necessary permissions, and cited accordingly.

Credit authorship contribution statement

Olivia K. Harrison: Project administration, Conceptualization, Writing – original draft, Writing – review & editing. **Xavier Guell:** Conceptualization, Writing – original draft, Writing – review & editing. **Miriam C. Klein-Flügge:** Conceptualization, Writing – original draft, Writing – review & editing. **Robert L. Barry:** Conceptualization, Writing – original draft, Writing – review & editing.

Acknowledgments

Three-dimensional representations of the amygdala, brainstem, cerebellum and spinal cord were made using ITK-SNAP www.itksnap.org (Yushkevich et al., 2006) and ParaView www.paraview.org (Ahrens et al., 2005). OKH (née Faull) was supported by a Rutherford Discovery Research Fellowship awarded by the Royal Society of New Zealand, and the School of Pharmacy at the University of Otago. XG was supported in part by the Massachusetts General Hospital Tosteson & Fund for Medical Discovery Award and La Caixa Banking Foundation (100010434, LCF/BQ/AN15/10380048). MCKF was supported by a Sir Henry Wellcome Fellowship (103184/Z/13/Z) and a Medical Research Council grant awarded to Matthew Rushworth (MR/P024955/1). RLB was supported by the United States National Institutes of Health (NIH) through grant R01EB027779. The content is solely the responsibility of the authors and does not necessarily represent the official views of the NIH. We would also like to thank the three reviewers for their constructive comments on this manuscript.

Supplementary materials

Supplementary material associated with this article can be found, in the online version, at doi:10.1016/j.neuroimage.2021.118379.

References

Adolphs, R., 2013. The Biology of Fear. Curr. Biol. 23 (2), R79–R93. doi:10.1016/j.cub.2012.11.055.
Aggarwal, M., Zhang, J., Pletnikova, O., Crain, B., Troncoso, J., Mori, S., 2013. Feasibility of creating a high-resolution 3D diffusion tensor imaging based atlas of the human brainstem: a case study at 11.7 T. Neuroimage 74, 117–127. doi:10.1016/j.neuroimage.2013.01.061.
Aggleton, J.P., 1993. The contribution of the amygdala to normal and abnormal emotional states. Trends Neurosci. 16 (8), 328–333. doi:10.1016/0166-2236(93)90110-8.
Aggleton, J.P., 2000. The Amygdala: A Functional Analysis. Oxford University Press.
Aggleton, J.P., Burton, M.J., Passingham, R.E., 1980. Cortical and subcortical afferents to the amygdala of the rhesus monkey (Macaca mulatta). Brain Res. 190 (2), 347–368. doi:10.1016/0006-8993(80)90279-6.
Aggleton, J.P., Wright, N.F., Rosene, D.L., Saunders, R.C., 2015. Complementary patterns of direct amygdala and hippocampal projections to the macaque prefrontal cortex. Cereb. Cortex 25 (11), 4351–4373. doi:10.1093/cercor/bhv019.
Ahrens, J., Geveci, B., Law, C., 2005. Visualization Handbook. Butterworth-Heinemann (pp. 717–LXXII). https://doi.org/ doi:10.1016/b978-012387582-2/50038-1.
Amaral, D.G., Price, J.L., 1984. Amygdalo-cortical projections in the monkey (Macaca fascicularis). J. Comp. Neurol. 230 (4), 465–496. doi:10.1002/cne.902300402.
Amaral, D.G., Price, J.L., Pitkanen, A., Carmichael, S.T., 1992. Anatomical organization of the primate amygdaloid complex. In: Aggleton, J.P. (Ed.), The Amygdala: Neurobiological Aspects of Emotion, Memory, and Mental Dysfunction. Wiley-Liss.
Anteraper, S.A., Guell, X., D'Mello, A., Joshi, N., Whitfield-Gabrieli, S., Joshi, G, 2019. Disrupted cerebrocerebellar intrinsic functional connectivity in young adults with high-functioning autism spectrum disorder: a data-driven, whole-brain, high-temporal resolution functional magnetic resonance imaging study. Brain Connect. 9 (1), 48–59. doi:10.1089/brain.2018.0581.
Bach, D.R., Behrens, T.E., Garrido, L., Weiskopf, N., Dolan, R.J., 2011. Deep and superficial amygdala nuclei projections revealed in vivo by probabilistic tractography. J. Neurosci. 31 (2), 618–623. doi:10.1523/jneurosci.2744-10.2011.
Balderston, N.L., Schultz, D.H., Hopkins, L., Helmstetter, F.J., 2015. Functionally distinct amygdala subregions identified using DTI and high-resolution fMRI. Soc. Cogn. Affect. Neurosci. 10 (12), 1615–1622. doi:10.1093/scan/nsv055.
Bär, K.J., de la Cruz, F., Schumann, A., Koehler, S., Sauer, H., Critchley, H., Wagner, G., 2016. Functional connectivity and network analysis of midbrain and brainstem nuclei. NeuroImage 134, 53–63. doi:10.1016/j.neuroimage.2016.03.071.
Barch, D.M., Burgess, G.C., Harms, M.P., Petersen, S.E., Schlaggar, B.L., Corbetta, M., Glasser, M.F., Curtiss, S., Dixit, S., Feldt, C., Nolan, D., Bryant, E., Hartley, T., Footer, O., Bjork, J.M., Poldrack, R., Smith, S., Johansen-Berg, H., Snyder, A.Z.WU-Minn HCP Consortium, 2013. Function in the human connectome: task-fMRI and individual differences in behavior. NeuroImage 80, 169–189. doi:10.1016/j.neuroimage.2013.05.033.

Barry, R.L., Conrad, B.N., Smith, S.A., Gore, J.C., 2018. A practical protocol for measurements of spinal cord functional connectivity. Sci. Rep. 8 (1), 16512. doi:10.1038/s41598-018-34841-6.
Barry, R.L., Rogers, B.P., Conrad, B.N., Smith, S.A., Gore, J.C., 2016. Reproducibility of resting state spinal cord networks in healthy volunteers at 7 Tesla. NeuroImage 133, 31–40. doi:10.1016/j.neuroimage.2016.02.058.
Barry, R.L., Smith, S.A., Dula, A.N., Gore, J.C., 2014. Resting state functional connectivity in the human spinal cord. ELife 3, e02812. doi:10.7554/elife.02812.
Barry, R.L., Vannesjo, S.J., By, S., Gore, J.C., Smith, S.A., 2018. Spinal cord MRI at 7T. NeuroImage 168, 437–451. doi:10.1016/j.neuroimage.2017.07.003.
Baur, V., Hänggi, J., Langer, N., Jäncke, L., 2013. Resting-state functional and structural connectivity within an insula–amygdala route specifically index state and trait anxiety. Biol. Psychiatry 73 (1), 85–92. doi:10.1016/j.biopsych.2012.06.003.
Beissner, F., 2015. Functional MRI of the brainstem: common problems and their solutions. Clin. Neuroradiol. 25 (Suppl 2), 251–257. doi:10.1007/s00062-015-0404-0.
Beissner, F., Schumann, A., Brunn, F., Eisenträger, D., Bär, K.-J., 2014. Advances in functional magnetic resonance imaging of the human brainstem. NeuroImage 86, 91–98. doi:10.1016/j.neuroimage.2013.07.081.
Bernard, J.A., Peltier, S.J., Benson, B.L., Wiggins, J.L., Jaeggi, S.M., Buschkuehl, M., Jonides, J., Monk, C.S., Seidler, R.D., 2014. Dissociable functional networks of the human dentate nucleus. Cereb. Cortex 24 (8), 2151–2159. doi:10.1093/cercor/bht065.
Bianciardi, M., Toschi, N., Edlow, B.L., Eichner, C., Setsompop, K., Polimeni, J.R., Brown, E.N., Kinney, H.C., Rosen, B.R., Wald, L.L., 2015. Toward an *in vivo* neuroimaging template of human brainstem nuclei of the ascending arousal, autonomic, and motor systems. Brain Connect. 5 (10), 597–607. doi:10.1089/brain.2015.0347.
Bianciardi, M., Toschi, N., Eichner, C., Polimeni, J.R., Setsompop, K., Brown, E.N., Hämäläinen, M.S., Rosen, B.R., Wald, L.L., 2016. *In vivo* functional connectome of human brainstem nuclei of the ascending arousal, autonomic, and motor systems by high spatial resolution 7-Tesla fMRI. Magn. Reson. Mater. Phys. Biol. Med. 29 (3), 451–462. doi:10.1007/s10334-016-0546-3.
Bickart, K.C., Hollenbeck, M.C., Barrett, L.F., Dickerson, B.C., 2012. Intrinsic amygdala-cortical functional connectivity predicts social network size in humans. J. Neurosci. 32 (42), 14729–14741. doi:10.1523/jneurosci.1599-12.2012.
Bielski, K., Adamus, S., Kolada, E., Leonardi, J.R., Szatkowska, I., 2021. Parcellation of the human amygdala using recurrence quantification analysis. NeuroImage 227, 117644. doi:10.1016/j.neuroimage.2020.117644.
Bijsterbosch, J., Ansari, T.L., Smith, S., Gauld, O., Zika, O., Boessenkool, S., Browning, M., Reinecke, A., Bishop, S.J., 2018. Stratification of MDD and GAD patients by resting state brain connectivity predicts cognitive bias. NeuroImage Clin. 19, 425–433. doi:10.1016/j.nicl.2018.04.033.
Bijsterbosch, J., Smith, S., Forster, S., John, O.P., Bishop, S.J., 2014. Resting state correlates of subdimensions of anxious affect. J. Cogn. Neurosci. 26 (4), 914–926. doi:10.1162/jocn_a_00512.
Biswal, B., Yetkin, F.Z., Haughton, V.M., Hyde, J.S., 1995. Functional connectivity in the motor cortex of resting human brain using echo-planar mri. Magn. Reson. Med. 34 (4), 537–541. doi:10.1002/mrm.1910340409.
Bostan, A.C., Dum, R.P., Strick, P.L., 2010. The basal ganglia communicate with the cerebellum. Proc. Natl. Acad. Sci. 107 (18), 8452–8456. doi:10.1073/pnas.1000496107.
Boubela, R.N., Kalcher, K., Huf, W., Seidel, E.M., Derntl, B., Pezawas, L., Našel, C., Moser, E., 2015. fMRI measurements of amygdala activation are confounded by stimulus correlated signal fluctuation in nearby veins draining distant brain regions. Sci. Rep. 5 (1), 10499. doi:10.1038/srep10499.
Brady, R.O., Gonsalvez, I., Lee, I., Öngür, D., Seidman, L.J., Schmahmann, J.D., Eack, S.M., Keshavan, M.S., Pascual-Leone, A., Halko, M.A., 2019. Cerebellar-prefrontal network connectivity and negative symptoms in schizophrenia. Am. J. Psychiatry 176 (7), 512–520. doi:10.1176/appi.ajp.2018.18040429.
Brodal, P., 1979. The pontocerebellar projection in the rhesus monkey: an experimental study with retrograde axonal transport of horseradish peroxidase. Neuroscience 4 (2), 193–208. doi:10.1016/0306-4522(79)90082-4.
Brooks, J.C.W., Faull, O.K., Pattinson, K.T.S., Jenkinson, M., 2013. Physiological noise in brainstem FMRI. Front. Hum. Neurosci. 7. doi:10.3389/fnhum.2013.00623, 623–13https://doi.org/.
Brown, V.M., LaBar, K.S., Haswell, C.C., Gold, A.L., Beall, S.K., Voorhees, E.V., Marx, C.E., Calhoun, P.S., Fairbank, J.A., Green, K.T., Tupler, L.A., Weiner, R.D., Beckham, J.C., Brancu, M., Hoerle, J.M., Pender, M., Kudler, H., Swinkels, C.M., Nieuwsma, J.A., Morey, R.A., 2014. Altered resting-state functional connectivity of basolateral and centromedial amygdala complexes in posttraumatic stress disorder. Neuropsychopharmacology 39 (2), 351–359. doi:10.1038/npp.2013.197.
Buckner, R.L., Krienen, F.M., Castellanos, A., Diaz, J.C., Yeo, B.T.T., 2011. The organization of the human cerebellum estimated by intrinsic functional connectivity. J. Neurophysiol. 106 (5), 2322–2345. doi:10.1152/jn.00339.2011.
By, S., Smith, A.K., Dethrage, L.M., Lyttle, B.D., Landman, B.A., Creasy, J.L., Pawate, S., Smith, S.A., 2016. Quantifying the impact of underlying measurement error on cervical spinal cord diffusion tensor imaging at 3T. J. Magn. Reson. Imaging 44 (6), 1608–1618. doi:10.1002/jmri.25308.
Bzdok, D., Laird, A.R., Zilles, K., Fox, P.T., Eickhoff, S.B., 2013. An investigation of the structural, connectional, and functional subspecialization in the human amygdala. Hum. Brain Mapp. 34 (12), 3247–3266. doi:10.1002/hbm.22138.
Cadotte, D.W., Cadotte, A., Cohen-Adad, J., Fleet, D., Livne, M., Wilson, J.R., Mikulis, D., Nugaeva, N., Fehlings, M.G., 2015. Characterizing the location of spinal and vertebral levels in the human cervical spinal cord. Am. J. Neuroradiol. 36 (4), 803–810. doi:10.3174/ajnr.a4192.
Carmichael, S.T., Price, J.L., 1995. Sensory and premotor connections of the orbital and medial prefrontal cortex of macaque monkeys. J. Comp. Neurol. 363 (4), 642–664. doi:10.1002/cne.903630409.
Catani, M., Howard, R.J., Pajevic, S., Jones, D.K., 2002. Virtual *in vivo* interactive dissection of white matter fasciculi in the human brain. NeuroImage 17 (1), 77–94. doi:10.1006/nimg.2002.1136.
Cerminara, N.L., Lang, E.J., Sillitoe, R.V., Apps, R., 2015. Redefining the cerebellar cortex as an assembly of non-uniform Purkinje cell microcircuits. Nat. Rev. Neurosci. 16 (2), 79–93. doi:10.1038/nrn3886.
Chang, L.J., Gianaros, P.J., Manuck, S.B., Krishnan, A., Wager, T.D., 2015. A sensitive and specific neural signature for picture-induced negative affect. PLoS Biol. 13 (6). doi:10.1371/journal.pbio.1002180, e1002180-28https://doi.org/.
Chen, L.M., Mishra, A., Yang, P.F., Wang, F., Gore, J.C., 2015. Injury alters intrinsic functional connectivity within the primate spinal cord. Proc. Natl. Acad. Sci. 112 (19), 5991–5996. doi:10.1073/pnas.1424106112.
Cheng, W., Rolls, E.T., Qiu, J., Xie, X., Lyu, W., Li, Y., Huang, C.C., Yang, A.C., Tsai, S.J., Lyu, F., Zhuang, K., Lin, C.P., Xie, P., Feng, J., 2018. Functional connectivity of the human amygdala in health and in depression. Soc. Cogn. Affect. Neurosci. 13 (6). doi:10.1093/scan/nsy032, nsy032-https://doi.org/.
Cho, Y.T., Ernst, M., Fudge, J.L., 2013. Cortico–amygdala-striatal circuits are organized as hierarchical subsystems through the primate amygdala. J. Neurosci. 33 (35), 14017–14030. doi:10.1523/jneurosci.0170-13.2013.
Chowdhury, R., Lambert, C., Dolan, R.J., Düzel, E., 2013. Parcellation of the human substantia nigra based on anatomical connectivity to the striatum. Neuroimage 81 (C), 191–198. doi:10.1016/j.neuroimage.2013.05.043.
Ciccarelli, O., Wheeler-Kingshott, C.A., McLean, M.A., Cercignani, M., Wimpey, K., Miller, D.H., Thompson, A.J., 2007. Spinal cord spectroscopy and diffusion-based tractography to assess acute disability in multiple sclerosis. Brain 130 (8), 2220–2231. doi:10.1093/brain/awm152.
Cohen-Adad, J., 2018. Microstructural imaging in the spinal cord and validation strategies. NeuroImage 182, 169–183. doi:10.1016/j.neuroimage.2018.04.009.
Cohen-Adad, J., Mendili, M.M.E., Morizot-Koutlidis, R., Lehéricy, S., Meininger, V., Blancho, S., Rossignol, S., Benali, H., Pradat, P.F., 2012. Involvement of spinal sensory pathway in ALS and specificity of cord atrophy to lower motor neuron degeneration. Amyotroph. Lateral Scler. Frontotemporal Degener. 14 (1), 30–38. doi:10.3109/17482968.2012.701308.
Connolly, C.G., Wu, J., Ho, T.C., Hoeft, F., Wolkowitz, O., Eisendrath, S., Frank, G., Hendren, R., Max, J.E., Paulus, M.P., Tapert, S.F., Banerjee, D., Simmons, A.N., Yang, T.T., 2013. Resting-state functional connectivity of subgenual anterior cingulate cortex in depressed adolescents. Biol. Psychiatry 74 (12), 898–907. doi:10.1016/j.biopsych.2013.05.036.
Conrad, B.N., Barry, R.L., Rogers, B.P., Maki, S., Mishra, A., Thukral, S., Sriram, S., Bhatia, A., Pawate, S., Gore, J.C., Smith, S.A., 2018. Multiple sclerosis lesions affect intrinsic functional connectivity of the spinal cord. Brain 141 (6), 1650–1664. doi:10.1093/brain/awy083.
Cowan, W.M., Gottlieb, D.I., Hendrickson, A.E., Price, J.L., Woolsey, T.A., 1972. The autoradiographic demonstration of axonal connections in the central nervous system. Brain Res. 37 (1), 21–51. doi:10.1016/0006-8993(72)90344-7.
Dauleac, C., Bannier, E., Cotton, F., Frindel, C., 2021. Effect of distortion corrections on the tractography quality in spinal cord diffusion-weighted imaging. Magn. Reson. Med. doi:10.1002/mrm.28665.
De Leener, B., Fonov, V.S., Collins, D.L., Callot, V., Stikov, N., Cohen-Adad, J., 2018. PAM50: Unbiased multimodal template of the brainstem and spinal cord aligned with the ICBM152 space. NeuroImage 165, 170–179. doi:10.1016/j.neuroimage.2017.10.041.
De Leener, B., Lévy, S., Dupont, S.M., Fonov, V.S., Stikov, N., Collins, D.L., Callot, V., Cohen-Adad, J., 2017. SCT: spinal cord toolbox, an open-source software for processing spinal cord MRI data. NeuroImage 145 (Pt A), 24–43. doi:10.1016/j.neuroimage.2016.10.009.
Diedrichsen, J., Zotow, E., 2015. Surface-based display of volume-averaged cerebellar imaging data. PLOS ONE 10 (7), e0133402. doi:10.1371/journal.pone.0133402.
Dietrichs, E., 1981. The cerebellar corticonuclear and nucleocortical projections in the cat as studied with anterograde and retrograde transport of horseradish peroxidase. Exp. Brain Res. 44 (3), 235–242. doi:10.1007/bf00236560.
Ding, S., Royall, J.J., Sunkin, S.M., Ng, L., Facer, B.A.C., Lesnar, P., Guillozet-Bongaarts, A., McMurray, B., Szafer, A., Dolbeare, T.A., Stevens, A., Tirrell, L., Benner, T., Caldejon, S., Dalley, R.A., Dee, N., Lau, C., Nyhus, J., Reding, M., LeinReference, E.S., 2017. Comprehensive cellular-resolution atlas of the adult human brain. J. Comp. Neurol. 525 (2). doi:10.1002/cne.24130, 407–407https://doi.org/.
D'Mello, A.M., Stoodley, C.J, 2015. Cerebro-cerebellar circuits in autism spectrum disorder. Front. Neurosci. 9, 408. doi:10.3389/fnins.2015.00408.
Doñamayor, N., Baek, K., Voon, V., 2017. Distal functional connectivity of known and emerging cortical targets for therapeutic noninvasive stimulation. Cereb. Cortex 28 (2), 791–804. doi:10.1093/cercor/bhx331.
Dong, D., Luo, C., Guell, X., Wang, Y., He, H., Duan, M., Eickhoff, S.B., Yao, D., 2020. Compression of cerebellar functional gradients in schizophrenia. Schizophr. Bull. 46 (5), 1282–1295. doi:10.1093/schbul/sbaa016.
Drevets, W.C., 2003. Neuroimaging Abnormalities in the Amygdala in mood disorders. Ann. N. Y. Acad. Sci. 985 (1), 420–444. doi:10.1111/j.1749-6632.2003.tb07098.x.
Dunckley, P., Wise, R.G., Fairhurst, M., Hobden, P., Aziz, Q., Chang, L., Tracey, I., 2005. A comparison of visceral and somatic pain processing in the human brainstem using functional magnetic resonance imaging. J. Neurosci. 25 (32), 7333–7341. doi:10.1523/jneurosci.1100-05.2005.
Duval, T., McNab, J.A., Setsompop, K., Witzel, T., Schneider, T., Huang, S.Y., Keil, B., Klawiter, E.C., Wald, L.L., Cohen-Adad, J., 2015. In vivo mapping of human spinal cord microstructure at 300mT/m. NeuroImage 118, 494–507. doi:10.1016/j.neuroimage.2015.06.038.
Edinger, L., 1896. Vorlesungen Über den Bau der nervösen Zentralorgane des Menschen und der Tiere. J. Nerv. Ment. Dis. 31 (8), 559.
Eippert, F., Kong, Y., Jenkinson, M., Tracey, I., Brooks, J.C.W., 2017. Denoising spinal

cord fMRI data: approaches to acquisition and analysis. NeuroImage 154, 255–266. doi:10.1016/j.neuroimage.2016.09.065.
Eippert, F., Kong, Y., Winkler, A.M., Andersson, J.L., Finsterbusch, J., Büchel, C., Brooks, J.C.W., Tracey, I., 2017. Investigating resting-state functional connectivity in the cervical spinal cord at 3T. NeuroImage 147, 589–601. doi:10.1016/j.neuroimage.2016.12.072.
Englot, D.J., Gonzalez, H.F.J., Reynolds, B.B., Konrad, P.E., Jacobs, M.L., Gore, J.C., Landman, B.A., Morgan, V.L., 2018. Relating structural and functional brainstem connectivity to disease measures in epilepsy. Neurology 91 (1), e67–e77. doi:10.1212/wnl.0000000000005733.
Eryilmaz, H., Ville, D.V.D., Schwartz, S., Vuilleumier, P., 2011. Impact of transient emotions on functional connectivity during subsequent resting state: A wavelet correlation approach. NeuroImage 54 (3), 2481–2491. doi:10.1016/j.neuroimage.2010.10.021.
Essen, D.C.V., Drury, H.A., Joshi, S., Miller, M.I., 1998. Functional and structural mapping of human cerebral cortex: Solutions are in the surfaces. Proc. Natl. Acad. Sci. 95 (3), 788–795. doi:10.1073/pnas.95.3.788.
Ezra, M., Faull, O.K., Jbabdi, S., Pattinson, K.T.S., 2015. Connectivity-based segmentation of the periaqueductal gray matter in human with brainstem optimized diffusion MRI. Hum. Brain Mapp. 36 (9), 3459–3471. doi:10.1002/hbm.22855.
Faull, O.K., Pattinson, K.T., 2017. The cortical connectivity of the periaqueductal gray and the conditioned response to the threat of breathlessness. ELife 6, e21749–e21767. doi:10.7554/elife.21749.
Felten, D.L., O'Banion, M.K., Maida, M.S., 2016. Elsevier. Netter's Atlas of Neuroscience (3rd ed.), Elsevier (pp. 51–70). doi:10.1016/b978-0-323-26511-9.00003-5
Finsterbusch, J., Sprenger, C., Büchel, C., 2013. Combined T2*-weighted measurements of the human brain and cervical spinal cord with a dynamic shim update. NeuroImage 79, 153–161. doi:10.1016/j.neuroimage.2013.04.021.
Flannigan, B.D., Bradley, W.G., Mazziotta, J.C., Rauschning, W., Bentson, J.R., Lufkin, R.B., Hieshima, G.B., 1985. Magnetic resonance imaging of the brainstem: normal structure and basic functional anatomy. Radiology 154 (2), 375–383. doi:10.1148/radiology.154.2.3966125.
Folloni, D., Sallet, J., Khrapitchev, A.A., Sibson, N., Verhagen, L., Mars, R.B., 2019. Dichotomous organization of amygdala/temporal-prefrontal bundles in both humans and monkeys. ELife 8, e47175. doi:10.7554/elife.47175.
Fonov, V.S., Troter, A.L., Taso, M., De Leener, B., Lévêque, G., Benhamou, M., Sdika, M., Benali, H., Pradat, P.-F., Collins, D.L., Callot, V., Cohen-Adad, J., 2014. Framework for integrated MRI average of the spinal cord white and gray matter: The MNI-Poly-AMU template. NeuroImage 102, 817–827. doi:10.1016/j.neuroimage.2014.08.057.
Fox, C.A., 1943. The stria terminalis, longitudinal association bundle and precommissural fornix fibers in the cat. J. Comp. Neurol. 79 (2), 277–295. doi:10.1002/cne.900790205.
Freedman, L.J., Insel, T.R., Smith, Y., 2000. Subcortical projections of area 25 (subgenual cortex) of the macaque monkey. J. Comp. Neurol. 421 (2), 172–188 https://doi.org/10.1002/(sici)1096-9861(20000529)421:2<172::aid-cne4>3.3.co;2-#.
Friedman, D.P., Aggleton, J.P., Saunders, R.C., 2002. Comparison of hippocampal, amygdala, and perirhinal projections to the nucleus accumbens: Combined anterograde and retrograde tracing study in the Macaque brain. J. Comp. Neurol. 450 (4), 345–365. doi:10.1002/cne.10336.
Fudge, J.L., Kunishio, K., Walsh, P., Richard, C., Haber, S.N., 2002. Amygdaloid projections to ventromedial striatal subterritories in the primate. Neuroscience 110 (2), 257–275. doi:10.1016/s0306-4522(01)00546-2.
Ghashghaei, H.T., Hilgetag, C.C., Barbas, H., 2007. Sequence of information processing for emotions based on the anatomic dialogue between prefrontal cortex and amygdala. NeuroImage 34 (3), 905–923. doi:10.1016/j.neuroimage.2006.09.046.
Glasser, M.F., Coalson, T.S., Robinson, E.C., Hacker, C.D., Harwell, J., Yacoub, E., Ugurbil, K., Andersson, J., Beckmann, C.F., Jenkinson, M., Smith, S.M., Essen, D.C.V., 2016. A multi-modal parcellation of human cerebral cortex. Nature 536 (7615), 171–178. doi:10.1038/nature18933.
Gloor, P., 1955. Electrophysiological studies on the connections of the amygdaloid nucleus in the cat Part I : The neuronal organization of the amygdaloid projection system. Electroencephalogr. Clin. Neurophysiol. 7 (2), 223–242. doi:10.1016/0013-4694(55)90037-7.
Glover, G.H., Li, T., Ress, D., 2000. Image-based method for retrospective correction of physiological motion effects in fMRI: RETROICOR. Magn. Reson. Med. 44 (1), 162–167 https://doi.org/10.1002/1522-2594(200007)44:1<162::aid-mrm23>3.0.co;2-e.
Gorka, A.X., Torrisi, S., Shackman, A.J., Grillon, C., Ernst, M., 2018. Intrinsic functional connectivity of the central nucleus of the amygdala and bed nucleus of the stria terminalis. NeuroImage 168, 392–402. doi:10.1016/j.neuroimage.2017.03.007.
Grabenhorst, F., Hernádi, I., Schultz, W., 2012. Prediction of economic choice by primate amygdala neurons. Proc. Natl. Acad. Sci. 109 (46), 18950–18955. doi:10.1073/pnas.1212706109.
Granziera, C., Schmahmann, J.D., Hadjikhani, N., Meyer, H., Meuli, R., Wedeen, V., Krueger, G., 2009. Diffusion spectrum imaging shows the structural basis of functional cerebellar circuits in the human cerebellum *in vivo*. PLoS ONE 4 (4), e5101. doi:10.1371/journal.pone.0005101.
Grayson, D.S., Bliss-Moreau, E., Machado, C.J., Bennett, J., Shen, K., Grant, K.A., Fair, D.A., Amaral, D.G., 2016. The rhesus monkey connectome predicts disrupted functional networks resulting from pharmacogenetic inactivation of the amygdala. Neuron 91 (2), 453–466. doi:10.1016/j.neuron.2016.06.005.
Griffanti, L., Douaud, G., Bijsterbosch, J., Evangelisti, S., Alfaro-Almagro, F., Glasser, M.F., Duff, E.P., Fitzgibbon, S., Westphal, R., Carone, D., Beckmann, C.F., Smith, S.M., 2017. Hand classification of fMRI ICA noise components. Neuroimage 154, 188–205. doi:10.1016/j.neuroimage.2016.12.036.
Guell, X., Anteraper, S.A., Gardner, A.J., Whitfield-Gabrieli, S., Kay-Lambkin, F., Iverson, G.L., Gabrieli, J., Stanwell, P., 2020a. Functional connectivity changes in retired rugby league players: a data-driven functional magnetic resonance imaging study. J. Neurotrauma 37 (16), 1788–1796. doi:10.1089/neu.2019.6782.
Guell, X., Anteraper, S.A., Ghosh, S.S., Gabrieli, J.D.E., Schmahmann, J.D., 2020b. Neurodevelopmental and psychiatric symptoms in patients with a cyst compressing the cerebellum: an ongoing enigma. Cerebellum 19 (1), 16–29. doi:10.1007/s12311-019-01050-4.
Guell, X., D'Mello, A.M., Hubbard, N.A., Romeo, R.R., Gabrieli, J.D.E., Whitfield-Gabrieli, S., Schmahmann, J.D., Anteraper, S.A, 2019. Functional territories of human dentate nucleus. Cereb. Cortex 30 (4), 2401–2417. doi:10.1093/cercor/bhz247.
Guell, X., Gabrieli, J.D.E., Schmahmann, J.D., 2018a. Embodied cognition and the cerebellum: Perspectives from the Dysmetria of Thought and the Universal Cerebellar Transform theories. Cortex 100, 140–148. doi:10.1016/j.cortex.2017.07.005.
Guell, X., Gabrieli, J.D.E., Schmahmann, J.D., 2018b. Triple representation of language, working memory, social and emotion processing in the cerebellum: convergent evidence from task and seed-based resting-state fMRI analyses in a single large cohort. NeuroImage 172, 437–449. doi:10.1016/j.neuroimage.2018.01.082.
Guell, X., Goncalves, M., Kaczmarzyk, J.R., Gabrieli, J.D.E., Schmahmann, J.D., Ghosh, S.S., 2019. LittleBrain: a gradient-based tool for the topographical interpretation of cerebellar neuroimaging findings. PLOS ONE 14 (1), e0210028. doi:10.1371/journal.pone.0210028.
Guell, X., Hoche, F., Schmahmann, J.D., 2015. Metalinguistic deficits in patients with cerebellar dysfunction: empirical support for the dysmetria of thought theory. Cerebellum 14 (1), 50–58. doi:10.1007/s12311-014-0630-z.
Guell, X., Schmahmann, J.D., 2020. Cerebellar Functional Anatomy: a Didactic Summary Based on Human fMRI Evidence. Cerebellum 19 (1), 1–5. doi:10.1007/s12311-019-01083-9.
Guell, X., Schmahmann, J.D., Gabrieli, J.D., Ghosh, S.S., 2018. Functional gradients of the cerebellum. ELife 7, e36652. doi:10.7554/elife.36652.
Guillery, R.W., 1995. Anatomical evidence concerning the role of the thalamus in corticocortical communication: a brief review. J Anat. 187 (Pt 3), 583–592.
Guo, C.C., Tan, R., Hodges, J.R., Hu, X., Sami, S., Hornberger, M., 2016. Network-selective vulnerability of the human cerebellum to Alzheimer's disease and frontotemporal dementia. Brain 139 (5), 1527–1538. doi:10.1093/brain/aww003.
Habas, C., Kamdar, N., Nguyen, D., Prater, K., Beckmann, C.F., Menon, V., Greicius, M.D., 2009. Distinct cerebellar contributions to intrinsic connectivity networks. J. Neurosci. 29 (26), 8586–8594. doi:10.1523/jneurosci.1868-09.2009.
Hahn, A., Stein, P., Windischberger, C., Weissenbacher, A., Spindelegger, C., Moser, E., Kasper, S., Lanzenberger, R., 2011. Reduced resting-state functional connectivity between amygdala and orbitofrontal cortex in social anxiety disorder. NeuroImage 56 (3), 881–889. doi:10.1016/j.neuroimage.2011.02.064.
Harita, S., Ioachim, G., Powers, J., Stroman, P.W., 2019. Investigation of resting-state BOLD networks in the human brainstem and spinal cord. Neuroscience 404, 71–81. doi:10.1016/j.neuroscience.2019.02.009.
Harita, S., Stroman, P.W., 2017. Confirmation of resting-state BOLD fluctuations in the human brainstem and spinal cord after identification and removal of physiological noise. Magn. Reson. Med. 78 (6), 2149–2156. doi:10.1002/mrm.26606.
Hoche, F., Guell, X., Sherman, J.C., Vangel, M.G., Schmahmann, J.D., 2016. Cerebellar contribution to social cognition. Cerebellum 15 (6), 732–743. doi:10.1007/s12311-015-0746-9.
Hoche, F., Guell, X., Vangel, M.G., Sherman, J.C., Schmahmann, J.D., 2018. The cerebellar cognitive affective/schmahmann syndrome scale. Brain 141 (1), 248–270. doi:10.1093/brain/awx317.
Holtzheimer, P.E., Husain, M.M., Lisanby, S.H., Taylor, S.F., Whitworth, L.A., McClintock, S., Slavin, K.V., Berman, J., McKhann, G.M., Patil, P.G., Rittberg, B.R., Abosch, A., Pandurangi, A.K., Holloway, K.L., Lam, R.W., Honey, C.R., Neimat, J.S., Henderson, J.M., DeBattista, C., …, Mayberg, H.S., 2017. Subcallosal cingulate deep brain stimulation for treatment-resistant depression: a multisite, randomised, sham-controlled trial. Lancet Psychiatry 4 (11), 839–849. doi:10.1016/s2215-0366(17)30371-1.
Hopkins, D.A., 1975. Amygdalotegmental projections in the rat, cat and rhesus monkey. Neurosci. Lett. 1 (5), 263–270. doi:10.1016/0304-3940(75)90041-5.
Hopkins, D.A., Holstege, G., 1978. Amygdaloid projections to the mesencephalon, pons and medulla oblongata in the cat. Exp. Brain Res. 32 (4), 529–547. doi:10.1007/bf00239551.
Horn, A., Ostwald, D., Reisert, M., Blankenburg, F., 2014. The structural-functional connectome and the default mode network of the human brain. NeuroImage 102, 142–151. doi:10.1016/j.neuroimage.2013.09.069.
Hoshi, E., Tremblay, L., Féger, J., Carras, P.L., Strick, P.L., 2005. The cerebellum communicates with the basal ganglia. Nat. Neurosci. 8 (11), 1491–1493. doi:10.1038/nn1544.
Hu, Y., Jin, R., Li, G., Luk, K.D., Wu, Ed.X., 2018. Robust spinal cord resting-state fMRI using independent component analysis-based nuisance regression noise reduction. J. Magn. Reson. Imaging 48 (5), 1421–1431. doi:10.1002/jmri.26048.
Ioachim, G., Powers, J.M., Stroman, P.W., 2019. Comparing coordinated networks across the brainstem and spinal cord in the resting state and altered cognitive state. Brain Connect. 9 (5), 415–424. doi:10.1089/brain.2018.0659.
Ioachim, G., Powers, J.M., Warren, H.J.M., Stroman, P.W., 2020. Coordinated human brainstem and spinal cord networks during the expectation of pain have elements unique from resting-state effects. Brain Sci. 10 (9), 568. doi:10.3390/brainsci10090568.
Irimia, A., Horn, J.D.V., 2021. Mapping the rest of the human connectome: atlasing the spinal cord and peripheral nervous system. NeuroImage 225, 117478. doi:10.1016/j.neuroimage.2020.117478.
Ito, M., 1993. Movement and thought: identical control mechanisms by the cerebellum. Trends Neurosci. 16 (11), 448–450. doi:10.1016/0166-2236(93)90073-u.
Ji, J.L., Spronk, M., Kulkarni, K., Repovš, G., Anticevic, A., Cole, M.W., 2019. Mapping

the human brain's cortical-subcortical functional network organization. NeuroImage 185, 35–57. doi:10.1016/j.neuroimage.2018.10.006.
Johansen-Berg, H., Gutman, D.A., Behrens, T.E.J., Matthews, P.M., Rushworth, M.F.S., Katz, E., Lozano, A.M., Mayberg, H.S., 2007. Anatomical connectivity of the subgenual cingulate region targeted with deep brain stimulation for treatment-resistant depression. Cereb. Cortex 18 (6), 1374–1383. doi:10.1093/cercor/bhm167.
Johnston, J.B., 1923. Further contributions to the study of the evolution of the forebrain. J. Comp. Neurol. 35 (5), 337–481. doi:10.1002/cne.900350502.
Kamali, A., Kramer, L.A., Frye, R.E., Butler, I.J., Hasan, K.M., 2010. Diffusion tensor tractography of the human brain cortico-ponto-cerebellar pathways: a quantitative preliminary study. J. Magn. Reson. Imaging 32 (4), 809–817. doi:10.1002/jmri.22330.
Kamali, A., Yousem, D.M., Lin, D.D., Sair, H.I., Jasti, S.P., Keser, Z., Riascos, R.F., Hasan, K.M., 2015. Mapping the trajectory of the stria terminalis of the human limbic system using high spatial resolution diffusion tensor tractography. Neurosci. Lett. 608, 45–50. doi:10.1016/j.neulet.2015.09.035.
Kandel, E.R., Schwartz, J.H., Jessell, T.M., 2000. Principles of Neural Science, Vol. 4. McGraw-hill.
Karavasilis, E., Christidi, F., Velonakis, G., Giavri, Z., Kelekis, N.L., Efstathopoulos, E.P., Evdokimidis, I., Dellatolas, G., 2019. Ipsilateral and contralateral cerebro-cerebellar white matter connections: a diffusion tensor imaging study in healthy adults. J. Neuroradiol. 46 (1), 52–60. doi:10.1016/j.neurad.2018.07.004.
Kelly, R.M., Strick, P.L., 2003. Cerebellar loops with motor cortex and prefrontal cortex of a nonhuman primate. J. Neurosci. 23 (23), 8432–8444. doi:10.1523/jneurosci.23-23-08432.2003.
Kelly, R.E., Alexopoulos, G.S., Wang, Z., Gunning, F.M., Murphy, C.F., Morimoto, S.S., Kanellopoulos, D., Jia, Z., Lim, K.O., Hoptman, M.J., 2010. Visual inspection of independent components: defining a procedure for artifact removal from fMRI data. J. Neurosci. Methods 189 (2), 233–245. doi:10.1016/j.jneumeth.2010.03.028.
Kerestes, R., Chase, H.W., Phillips, M.L., Ladouceur, C.D., Eickhoff, S.B., 2017. Multimodal evaluation of the amygdala's functional connectivity. NeuroImage 148, 219–229. doi:10.1016/j.neuroimage.2016.12.023.
Keuken, M.C., Bazin, P.L., Crown, L., Hootsmans, J., Laufer, A., Müller-Axt, C., Sier, R., van der Putten, E.J., Schäfer, A., Turner, R., Forstmann, B.U., 2014. Quantifying inter-individual anatomical variability in the subcortex using 7T structural MRI. NeuroImage 94, 40–46. doi:10.1016/j.neuroimage.2014.03.032.
Kim, M.J., Gee, D.G., Loucks, R.A., Davis, F.C., Whalen, P.J., 2011. Anxiety dissociates dorsal and ventral medial prefrontal cortex functional connectivity with the amygdala at rest. Cereb. Cortex 21 (7), 1667–1673. doi:10.1093/cercor/bhq237.
Kinany, N., Pirondini, E., Micera, S., Ville, D.V.D., 2020. Dynamic functional connectivity of resting-state spinal cord fMRI reveals fine-grained intrinsic architecture. Neuron 108 (3), 424–435. doi:10.1016/j.neuron.2020.07.024, e4https://doi.org/.
King, M., Hernandez-Castillo, C.R., Poldrack, R.A., Ivry, R.B., Diedrichsen, J., 2019. Functional boundaries in the human cerebellum revealed by a multi-domain task battery. Nat. Neurosci. 22 (8), 1371–1378. doi:10.1038/s41593-019-0436-x.
Klein-Flügge, M.C., Jensen, D.E.A., Takagi, Y., Verhagen, L., Smith, S.M., Rushworth, M.F.S., 2020. Anatomically precise relationship between specific amygdala connections and selective markers of mental well-being in humans. BioRxiv doi:10.1101/2020.03.08.980995, 03.08.980995https://doi.org/.
Klein-Flügge, M.C., Wittmann, M.K., Shpektor, A., Jensen, D.E.A., Rushworth, M.F.S., 2019. Multiple associative structures created by reinforcement and incidental statistical learning mechanisms. Nat. Commun. 10 (1), 4835. doi:10.1038/s41467-019-12557-z.
Koller, K., Hatton, C.M., Rogers, R.D., Rafal, R.D., 2019. Stria terminalis microstructure in humans predicts variability in orienting towards threat. Eur. J. Neurosci. 50 (11), 3804–3813. doi:10.1111/ejn.14504.
Kong, Y., Eippert, F., Beckmann, C.F., Andersson, J., Finsterbusch, J., Büchel, C., Tracey, I., Brooks, J.C.W., 2014. Intrinsically organized resting state networks in the human spinal cord. Proc. Natl. Acad. Sci. 111 (50), 18067–18072. doi:10.1073/pnas.1414293111.
Krettek, J.E., Price, J.L., 1978. Amygdaloid projections to subcortical structures within the basal forebrain and brainstem in the rat and cat. J. Comp. Neurol. 178 (2), 225–253. doi:10.1002/cne.901780204.
Kristensson, K., Olsson, Y., 1971. Uptake and retrograde axonal transport of peroxidase in hypoglossal neurones. Acta Neuropathol. 19 (1), 1–9. doi:10.1007/bf00690948.
Kundu, P., Inati, S.J., Evans, J.W., Luh, W.M., Bandettini, P.A., 2012. Differentiating BOLD and non-BOLD signals in fMRI time series using multi-echo EPI. NeuroImage 60 (3), 1759–1770. doi:10.1016/j.neuroimage.2011.12.028.
Kundu, P., Voon, V., Balchandani, P., Lombardo, M.V., Poser, B.A., Bandettini, P.A., 2017. Multi-echo fMRI: a review of applications in fMRI denoising and analysis of BOLD signals. NeuroImage 154, 59–80. doi:10.1016/j.neuroimage.2017.03.033.
Lee, Y.J., Guell, X., Hubbard, N.A., Siless, V., Frosch, I.R., Goncalves, M., Lo, N., Nair, A., Ghosh, S.S., Hofmann, S.G., Auerbach, R.P., Pizzagalli, D.A., Yendiki, A., Gabrieli, J.D.E., Whitfield-Gabrieli, S., Anteraper, S.A., 2020. Functional alterations in cerebellar functional connectivity in anxiety disorders. Cerebellum 1–10. doi:10.1007/s12311-020-01213-8.
Leitner, Y., Travis, K.E., Ben-Shachar, M., Yeom, K.W., Feldman, H.M., 2015. Tract profiles of the cerebellar white matter pathways in children and adolescents. Cerebellum 14 (6), 613–623. doi:10.1007/s12311-015-0652-1.
Liu, X., Qian, W., Jin, R., Li, X., Luk, K.D., Wu, Ed.X., Hu, Y., 2016. Amplitude of low frequency fluctuation (ALFF) in the cervical spinal cord with stenosis: a resting state fMRI study. PLOS ONE 11 (12), e0167279. doi:10.1371/journal.pone.0167279.
Liu, X., Zhou, F., Li, X., Qian, W., Cui, J., Zhou, I.Y., Luk, K.D.K., Wu, Ed.X., Hu, Y., 2016. Organization of the intrinsic functional network in the cervical spinal cord: a resting state functional MRI study. Neuroscience 336, 30–38. doi:10.1016/j.neuroscience.2016.08.042.
Logothetis, N.K., Wandell, B.A., 2004. Interpreting the BOLD Signal. Annu. Rev. Physiol. 66 (1), 735–769. doi:10.1146/annurev.physiol.66.082602.092845.
Mai, J.K., Majtanik, M., Paxinos, G., 2015. Atlas of the Human Brain. Academic Press.
Mars, R.B., Sallet, J., Neubert, F.X., Rushworth, M.F.S., 2013. Connectivity profiles reveal the relationship between brain areas for social cognition in human and monkey temporoparietal cortex. Proc. Natl. Acad. Sci. 110 (26), 10806–10811. doi:10.1073/pnas.1302956110.
Martucci, K.T., Weber, K.A., Mackey, S.C., 2019. Altered cervical spinal cord resting-state activity in fibromyalgia. Arthritis Rheumatol. 71 (3), 441–450. doi:10.1002/art.40746.
Massire, A., Rasoanandrianina, H., Taso, M., Guye, M., Ranjeva, J., Feiweier, T., Callot, V., 2018. Feasibility of single-shot multi-level multi-angle diffusion tensor imaging of the human cervical spinal cord at 7T. Magn. Reson. Med. 80 (3), 947–957. doi:10.1002/mrm.27087.
Massire, A., Taso, M., Besson, P., Guye, M., Ranjeva, J.-P., Callot, V., 2016. High-resolution multi-parametric quantitative magnetic resonance imaging of the human cervical spinal cord at 7T. NeuroImage 143, 58–69. doi:10.1016/j.neuroimage.2016.08.055.
Mayberg, H.S., Lozano, A.M., Voon, V., McNeely, H.E., Seminowicz, D., Hamani, C., Schwalb, J.M., Kennedy, S.H., 2005. Deep brain stimulation for treatment-resistant depression. Neuron 45 (5), 651–660. doi:10.1016/j.neuron.2005.02.014.
McFadyen, J., Mattingley, J.B., Garrido, M.I., 2019. An afferent white matter pathway from the pulvinar to the amygdala facilitates fear recognition. ELife 8, e40766. doi:10.7554/elife.40766.
Middleton, F., Strick, P., 1994. Anatomical evidence for cerebellar and basal ganglia involvement in higher cognitive function. Science 266 (5184), 458–461. doi:10.1126/science.7939688.
Monte, O.D., Costa, V.D., Noble, P.L., Murray, E.A., Averbeck, B.B., 2015. Amygdala lesions in rhesus macaques decrease attention to threat. Nat. Commun. 6 (1), 10161. doi:10.1038/ncomms10161.
Mori, S., Oishi, K., Faria, A.V., 2009. White matter atlases based on diffusion tensor imaging. Curr. Opin. Neurol. 22 (4), 362–369. doi:10.1097/wco.0b013e32832d954b.
Mori, S., Oishi, K., Jiang, H., Jiang, L., Li, X., Akhter, K., Hua, K., Faria, A.V., Mahmood, A., Woods, R., Toga, A.W., Pike, G.B., Neto, P.R., Evans, A., Zhang, J., Huang, H., Miller, M.I., van Zijl, P., Mazziotta, J., 2008. Stereotaxic white matter atlas based on diffusion tensor imaging in an ICBM template. Neuroimage 40 (2), 570–582. doi:10.1016/j.neuroimage.2007.12.035.
Murray, E.A., Wise, S.P., 2010. Interactions between orbital prefrontal cortex and amygdala: advanced cognition, learned responses and instinctive behaviors. Curr. Opin. Neurobiol. 20 (2), 212–220. doi:10.1016/j.conb.2010.02.001.
Murray, E.A., Wise, S.P., Drevets, W.C., 2011. Localization of dysfunction in major depressive disorder: prefrontal cortex and amygdala. Biol. Psychiatry 69 (12), e43–e54. doi:10.1016/j.biopsych.2010.09.041.
Naidich, T.P., Duvernoy, H.M., Delman, B.N., Sorensen, A.G., Kollias, S.S., Haacke, E.M., 2009. Duvernoy's Atlas of the Human Brain Stem and Cerebellum. Springer Science & Business Media doi:10.1007/978-3-211-73971-6.
Neubert, F.X., Mars, R.B., Thomas, A.G., Sallet, J., Rushworth, M.F.S., 2014. Comparison of human ventral frontal cortex areas for cognitive control and language with areas in monkey frontal cortex. Neuron 81 (3), 700–713. doi:10.1016/j.neuron.2013.11.012.
Niu, J., Ding, L., Li, J.J., Kim, H., Liu, J., Li, H., Moberly, A., Badea, T.C., Duncan, I.D., Son, Y.J., Scherer, S.S., Luo, W., 2013. Modality-based organization of ascending somatosensory axons in the direct dorsal column pathway. J. Neurosci. 33 (45), 17691–17709. doi:10.1523/jneurosci.3429-13.2013.
Nord, C.L., Gray, A., Robinson, O.J., Roiser, J.P., 2019. Reliability of fronto-amygdala coupling during emotional face processing. Brain Sci. 9 (4), 89. doi:10.3390/brainsci9040089.
Oler, J.A., Birn, R.M., Patriat, R., Fox, A.S., Shelton, S.E., Burghy, C.A., Stodola, D.E., Essex, M.J., Davidson, R.J., Kalin, N.H., 2012. Evidence for coordinated functional activity within the extended amygdala of non-human and human primates. NeuroImage 61 (4), 1059–1066. doi:10.1016/j.neuroimage.2012.03.045.
Oler, J.A., Tromp, D.P.M., Fox, A.S., Kovner, R., Davidson, R.J., Alexander, A.L., McFarlin, D.R., Birn, R.M., Berg, B.E., deCampo, D.M., Kalin, N.H., Fudge, J.L., 2017. Connectivity between the central nucleus of the amygdala and the bed nucleus of the stria terminalis in the non-human primate: neuronal tract tracing and developmental neuroimaging studies. Brain Struct. Funct. 222 (1), 21–39. doi:10.1007/s00429-016-1198-9.
O'Reilly, J.X., Croxson, P.L., Jbabdi, S., Sallet, J., Noonan, M.P., Mars, R.B., Browning, P.G.F., Wilson, C.R.E., Mitchell, A.S., Miller, K.L., Rushworth, M.F.S., Baxter, M.G., 2013. Causal effect of disconnection lesions on interhemispheric functional connectivity in rhesus monkeys. Proc. Natl. Acad. Sci. 110 (34), 13982–13987. doi:10.1073/pnas.1305062110.
Park, A.T., Leonard, J.A., Saxler, P., Cyr, A.B., Gabrieli, J.D.E., Mackey, A.P., 2018. Amygdala-medial prefrontal connectivity relates to stress and mental health in early childhood. Soc. Cogn. Affect. Neurosci. 13 (4). doi:10.1093/scan/nsy017, nsy017-https://doi.org/.
Paxinos, G., Huang, X.F., 2013. Atlas of the Human Brainstem. Elsevier doi:10.1016/b978-0-08-092521-9.50003-2.
Pelzer, E.A., Hintzen, A., Goldau, M., Cramon, D.Y., Timmermann, L., Tittgemeyer, M., 2013. Cerebellar networks with basal ganglia: feasibility for tracking cerebello-pallidal and subthalamo-cerebellar projections in the human brain. Eur. J. Neurosci. 38 (8), 3106–3114. doi:10.1111/ejn.12314.
Phelps, E.A., LeDoux, J.E., 2005. Contributions of the amygdala to emotion processing: from animal models to human behavior. Neuron 48 (2), 175–187. doi:10.1016/j.neuron.2005.09.025.
Plantinga, B.R., Roebroeck, A., Kemper, V.G., Uludağ, K., Melse, M., Mai, J., Kuijf, M.L., Herrler, A., Jahanshahi, A., Romeny, B.M., ter, H., Temel, Y., 2016. Ultra-high field mri post mortem structural connectivity of the human subthala-

mic nucleus, substantia nigra, and globus pallidus. Front. Neuroanat. 10 (26). doi:10.3389/fnana.2016.00066, 117–10https://doi.org/.
Price, J.L., 2003. Comparative aspects of amygdala connectivity. Ann. N. Y. Acad. Sci. 985 (1), 50–58. doi:10.1111/j.1749-6632.2003.tb07070.x.
Price, J.L., Amaral, D.G., 1981. An autoradiographic study of the projections of the central nucleus of the monkey amygdala. J. Neurosci. 1 (11), 1242–1259. doi:10.1523/jneurosci.01-11-01242.1981.
Price, J.L., Drevets, W.C., 2010. Neurocircuitry of mood disorders. Neuropsychopharmacology 35 (1), 192–216. doi:10.1038/npp.2009.104.
Pruessmann, K.P., Weiger, M., Scheidegger, M.B., Boesiger, P., 1999. SENSE: Sensitivity encoding for fast MRI. Magn. Reson. Med. 42 (5), 952–962 https://doi.org/10.1002/(sici)1522-2594(199911)42:5<952::aid-mrm16>3.0.co;2-s.
Pruim, R.H.R., Mennes, M., van Rooij, D., Llera, A., Buitelaar, J.K., Beckmann, C.F., 2015. ICA-AROMA: a robust ICA-based strategy for removing motion artifacts from fMRI data. NeuroImage 112, 267–277. doi:10.1016/j.neuroimage.2015.02.064.
Purves, D., Augustine, G.J., Fitzpatrick, D., Hall, W.C., LaMantia, A.S., White, L.E., 2011. Neuroscience. Sinauer Associates, Inc.
Ramnani, N., 2006. The primate cortico-cerebellar system: anatomy and function. Nat. Rev. Neurosci. 7 (7), 511–522. doi:10.1038/nrn1953.
Robinson, S., Windischberger, C., Rauscher, A., Moser, E., 2004. Optimized 3 T EPI of the amygdalae. NeuroImage 22 (1), 203–210. doi:10.1016/j.neuroimage.2003.12.048.
Robson, P.M., Grant, A.K., Madhuranthakam, A.J., Lattanzi, R., Sodickson, D.K., McKenzie, C.A., 2008. Comprehensive quantification of signal-to-noise ratio and g-factor for image-based and k-space-based parallel imaging reconstructions. Magn. Reson. Med. 60 (4), 895–907. doi:10.1002/mrm.21728.
Roy, A.K., Shehzad, Z., Margulies, D.S., Kelly, A.M.C., Uddin, L.Q., Gotimer, K., Biswal, B.B., Castellanos, F.X., Milham, M.P., 2009. Functional connectivity of the human amygdala using resting state fMRI. NeuroImage 45 (2), 614–626. doi:10.1016/j.neuroimage.2008.11.030.
Salimi-Khorshidi, G., Douaud, G., Beckmann, C.F., Glasser, M.F., Griffanti, L., Smith, S.M., 2014. Automatic denoising of functional MRI data: Combining independent component analysis and hierarchical fusion of classifiers. Neuroimage 90 (C), 449–468. doi:10.1016/j.neuroimage.2013.11.046.
Sallet, J., Mars, R.B., Noonan, M.P., Neubert, F.X., Jbabdi, S., O'Reilly, J.X., Filippini, N., Thomas, A.G., Rushworth, M.F., 2013. The organization of dorsal frontal cortex in humans and macaques. J. Neurosci. 33 (30), 12255–12274. doi:10.1523/jneurosci.5108-12.2013.
San Emeterio Nateras, O., Yu, F., Muir, E.R., III, C.B., Franklin, C.G., Li, W., Li, J., Lancaster, J.L., Duong, T.Q., 2015. Intrinsic resting-state functional connectivity in the human spinal cord at 3.0 T. Radiology 279 (1), 262–268. doi:10.1148/radiol.2015150768.
Santarelli, X., Garbin, G., Ukmar, M., Longo, R., 2010. Dependence of the fractional anisotropy in cervical spine from the number of diffusion gradients, repeated acquisition and voxel size. Magn. Reson. Imaging 28 (1), 70–76. doi:10.1016/j.mri.2009.05.046.
van der Saygin, Z.M., Kliemann, D., Iglesias, J.E., Kouwe, A.J.W., Boyd, E., Reuter, M., Stevens, A., Leemput, K.V., McKee, A., Frosch, M.P., Fischl, B., Augustinack, J.C.Alzheimer's Disease Neuroimaging Initiative, 2017. High-resolution magnetic resonance imaging reveals nuclei of the human amygdala: manual segmentation to automatic atlas. NeuroImage 155, 370–382. doi:10.1016/j.neuroimage.2017.04.046.
Schmahmann, J.D., 1996. From movement to thought: anatomic substrates of the cerebellar contribution to cognitive processing. Hum. Brain Mapp. 4 (3), 174–198. doi:10.1002/(sici)1097-0193(1996)4:3<174::aid-hbm3>3.0.co;2-0.
Schmahmann, J.D., 2000. The role of the cerebellum in affect and psychosis. J. Neurolinguist. 13 (2–3), 189–214. doi:10.1016/s0911-6044(00)00011-7.
Schmahmann, J.D., 2001. The cerebrocerebellar system: anatomic substrates of the cerebellar contribution to cognition and emotion. Int. Rev. Psychiatry 13 (4), 247–260. doi:10.1080/09540260127525.
Schmahmann, J.D., 2004. Disorders of the Cerebellum: Ataxia, Dysmetria of Thought, and the Cerebellar Cognitive Affective Syndrome. J. Neuropsychiatry Clin. Neurosci. 16 (3), 367–378. doi:10.1176/jnp.16.3.367.
Schmahmann, J.D., Pandya, D.N., 1989. Anatomical investigation of projections to the basis pontis from posterior parietal association cortices in rhesus monkey. J. Comp. Neurol. 289, 53–73. https://onlinelibrary.wiley.com/doi/pdf/10.1002/cne.903080209?casa_token=MAacgsFyU2UAAAAA:WhACj3UtagkXKNcTgr9-Syi0YNY0XJsbf14wjnSoxzkZg7f1KdkuZcoyMKKKKDR2j-JxKXrRNEF1lR_Y.
Schmahmann, J.D., Pandya, D.N., 1991. Projections to the basis pontis from the superior temporal sulcus and superior temporal region in the rhesus monkey. Journal of Comparative Neurology 308 (2), 224–248. doi:10.1002/cne.903080209.
Schmahmann, J.D., Pandya, D.N., 1993. Prelunate, occipitotemporal, and parahippocampal projections to the basis pontis in rhesus monkey. J. Comp. Neurol. 337 (1), 94–112. doi:10.1002/cne.903370107.
Schmahmann, J.D., Pandya, D.N., 1997. The cerebrocerebellar system. Int. Rev. Neurobiol. 41, 31–60. doi:10.1016/s0074-7742(08)60346-3.
Schmahmann, J.D., Rosene, D.L., Pandya, D.N., 2004. Motor projections to the basis pontis in rhesus monkey. J. Comp. Neurol. 478 (3), 248–268. doi:10.1002/cne.20286.
Schmahmann, J.D., Sherman, J.C., 1998. The cerebellar cognitive affective syndrome. Brain 121 (4), 561–579. doi:10.1093/brain/121.4.561.
Schmahmann, J.D., Weilburg, J.B., Sherman, J.C., 2007. The neuropsychiatry of the cerebellum-insights from the clinic. Cerebellum 6 (3), 254–267. doi:10.1080/14734220701490995.
Sclocco, R., Beissner, F., Bianciardi, M., Polimeni, J.R., Napadow, V., 2018. Challenges and opportunities for brainstem neuroimaging with ultrahigh field MRI. Neuroimage 168, 412–426. doi:10.1016/j.neuroimage.2017.02.052.
Smith, S.M., Beckmann, C.F., Andersson, J., Auerbach, E.J., Bijsterbosch, J., Douaud, G., Duff, E., Feinberg, D.A., Griffanti, L., Harms, M.P., Kelly, M., Laumann, T., Miller, K.L., Moeller, S., Petersen, S., Power, J., Salimi-Khorshidi, G., Snyder, A.Z., Vu, A.T.WU-Minn HCP Consortium, 2013. Resting-state fMRI in the human connectome project. NeuroImage 80, 144–168. doi:10.1016/j.neuroimage.2013.05.039.
Solano-Castiella, E., Anwander, A., Lohmann, G., Weiss, M., Docherty, C., Geyer, S., Reimer, E., Friederici, A.D., Turner, R., 2010. Diffusion tensor imaging segments the human amygdala in vivo. NeuroImage 49 (4), 2958–2965. doi:10.1016/j.neuroimage.2009.11.027.
Sprenger, C., Finsterbusch, J., Büchel, C., 2015. Spinal cord–midbrain functional connectivity is related to perceived pain intensity: a combined spino-cortical fMRI study. J. Neurosci. 35 (10), 4248–4257. doi:10.1523/jneurosci.4897-14.2015.
Steele, C.J., Anwander, A., Bazin, P.L., Trampel, R., Schaefer, A., Turner, R., Ramnani, N., Villringer, A., 2016. Human cerebellar sub-millimeter diffusion imaging reveals the motor and non-motor topography of the dentate nucleus. Cereb. Cortex doi:10.1093/cercor/bhw258.
Stefanacci, L., Amaral, D.G., 2002. Some observations on cortical inputs to the macaque monkey amygdala: An anterograde tracing study. J. Comp. Neurol. 451 (4), 301–323. doi:10.1002/cne.10339.
Steward, O., 2000. Functional Neuroscience. Springer, pp. 485–495. doi:10.1007/978-1-4612-1198-3_30.
Stieltjes, B., Kaufmann, W.E., Zijl, P.C., van, Fredericksen, K., Pearlson, G.D., Solaiyappan, M., Mori, S., 2001. Diffusion tensor imaging and axonal tracking in the human brainstem. Neuroimage 14 (3), 723–735. doi:10.1006/nimg.2001.0861.
Takahashi, E., Song, J.W., Folkerth, R.D., Grant, P.E., Schmahmann, J.D., 2013. Detection of postmortem human cerebellar cortex and white matter pathways using high angular resolution diffusion tractography: a feasibility study. NeuroImage 68, 105–111. doi:10.1016/j.neuroimage.2012.11.042.
Thomas, C.G., Harshman, R.A., Menon, R.S., 2002. Noise reduction in BOLD-Based fMRI using component analysis. NeuroImage 17 (3), 1521–1537. doi:10.1006/nimg.2002.1200.
Tian, Y., Margulies, D.S., Breakspear, M., Zalesky, A., 2020. Topographic organization of the human subcortex unveiled with functional connectivity gradients. Nat. Neurosci. 23 (11), 1421–1432. doi:10.1038/s41593-020-00711-6.
Tinnermann, A., Geuter, S., Sprenger, C., Finsterbusch, J., Büchel, C., 2017. Interactions between brain and spinal cord mediate value effects in nocebo hyperalgesia. Science 358 (6359), 105–108. doi:10.1126/science.aan1221.
Tinnermann, A., Büchel, C., Cohen-Adad, J., 2020. Cortico-spinal imaging to study pain. NeuroImage 224, 117439. doi:10.1016/j.neuroimage.2020.117439.
Toescu, S.M., Hales, P.W., Kaden, E., Lacerda, L.M., Aquilina, K., Clark, C.A., 2020. Tractographic and microstructural analysis of the dentato-rubro-thalamo-cortical tracts in children using diffusion MRI. Cereb. Cortex doi:10.1093/cercor/bhaa377, bhaa377-https://doi.org/.
Uğurbil, K., Xu, J., Auerbach, E.J., Moeller, S., Vu, A.T., Duarte-Carvajalino, J.M., Lenglet, C., Wu, X., Schmitter, S., de Moortele, P.F.V., Strupp, J., Sapiro, G., Martino, F.D., Wang, D., Harel, N., Garwood, M., Chen, L., Feinberg, D.A., Smith, S.M.WU-Minn HCP Consortium, 2013. Pushing spatial and temporal resolution for functional and diffusion MRI in the human connectome project. NeuroImage 80, 80–104. doi:10.1016/j.neuroimage.2013.05.012.
Vahdat, S., Khatibi, A., Lungu, O., Finsterbusch, J., Büchel, C., Cohen-Adad, J., Marchand-Pauvert, V., Doyon, J., 2020. Resting-state brain and spinal cord networks in humans are functionally integrated. PLOS Biol. 18 (7), e3000789. doi:10.1371/journal.pbio.3000789.
van Marle, H.J.F., Hermans, E.J., Qin, S., Fernández, G., 2010. Enhanced resting-state connectivity of amygdala in the immediate aftermath of acute psychological stress. NeuroImage 53 (1), 348–354. doi:10.1016/j.neuroimage.2010.05.070.
Veer, I.M., Beckmann, C.F., van Tol, M.J., Ferrarini, L., Milles, J., Veltman, D.J., Aleman, A., van Buchem, M.A., van der Wee, N.J., Rombouts, S.A.R.B., 2010. Whole brain resting-state analysis reveals decreased functional connectivity in major depression. Frontiers in Systems Neuroscience 4, 41. doi:10.3389/fnsys.2010.00041.
Veer, I.M., Oei, N.Y.L., Spinhoven, P., Buchem, M.A.van, Elzinga, B.M., Rombouts, S.A.R.B., 2011. Beyond acute social stress: Increased functional connectivity between amygdala and cortical midline structures. NeuroImage 57 (4), 1534–1541. doi:10.1016/j.neuroimage.2011.05.074.
Veer, I.M., Oei, N.Y.L., Spinhoven, P., Buchem, M.A.van, Elzinga, B.M., Rombouts, S.A.R.B., 2012. Endogenous cortisol is associated with functional connectivity between the amygdala and medial prefrontal cortex. Psychoneuroendocrinology 37 (7), 1039–1047. doi:10.1016/j.psyneuen.2011.12.001.
Voogd, J., Glickstein, M., 1998. The anatomy of the cerebellum. Trends Cogn. Sci. 2 (9), 307–313. doi:10.1016/s1364-6613(98)01210-8.
Vu, A.T., Jamison, K., Glasser, M.F., Smith, S.M., Coalson, T., Moeller, S., Auerbach, E.J., Uğurbil, K., Yacoub, E., 2017. Tradeoffs in pushing the spatial resolution of fMRI for the 7T Human Connectome Project. NeuroImage 154, 23–32. doi:10.1016/j.neuroimage.2016.11.049.
Wagner, G., de la Cruz, F., Köhler, S., Bär, K.J., 2017. Treatment associated changes of functional connectivity of midbrain/brainstem nuclei in major depressive disorder. Sci. Rep. 7 (1), 8675. doi:10.1038/s41598-017-09077-5.
Weber, K.A., Sentis, A.I., Bernadel-Huey, O.N., Chen, Y., Wang, X., Parrish, T.B., Mackey, S., 2018. Thermal stimulation alters cervical spinal cord functional connectivity in humans. Neuroscience 369, 40–50. doi:10.1016/j.neuroscience.2017.10.035.
Wei, P., Li, J., Gao, F., Ye, D., Zhong, Q., Liu, S., 2009. Resting state networks in human cervical spinal cord observed with fMRI. Eur. J. Appl. Physiol. 108 (2), 265. doi:10.1007/s00421-009-1205-4.
Weis, C.N., Huggins, A.A., Bennett, K.P., Parisi, E.A., Larson, C.L., 2019. High-resolution

resting-state functional connectivity of the extended amygdala. Brain Connect. 9 (8), 627–637. doi:10.1089/brain.2019.0688.

Workman, C.I., Lythe, K.E., McKie, S., Moll, J., Gethin, J.A., Deakin, J.F., Elliott, R., Zahn, R., 2016. Subgenual cingulate-amygdala functional disconnection and vulnerability to melancholic depression. Neuropsychopharmacology 41 (8), 2082–2090. doi:10.1038/npp.2016.8.

Wu, T.L., Byun, N.E., Wang, F., Mishra, A., Janve, V.A., Chen, L.M., Gore, J.C., 2020. Longitudinal assessment of recovery after spinal cord injury with behavioral measures and diffusion, quantitative magnetization transfer and functional magnetic resonance imaging. NMR Biomed. 33 (4), e4216. doi:10.1002/nbm.4216.

Wu, T.L., Wang, F., Mishra, A., Wilson, G.H., Byun, N., Chen, L.M., Gore, J.C., 2018. Resting-state functional connectivity in the rat cervical spinal cord at 9.4 T. Magn. Reson. Med. 79 (5), 2773–2783. doi:10.1002/mrm.26905.

Wu, T.L., Yang, P.F., Wang, F., Shi, Z., Mishra, A., Wu, R., Chen, L.M., Gore, J.C., 2019. Intrinsic functional architecture of the non-human primate spinal cord derived from fMRI and electrophysiology. Nat. Commun. 10 (1), 1416. doi:10.1038/s41467-019-09485-3.

Yushkevich, P.A., Piven, J., Hazlett, H.C., Smith, R.G., Ho, S., Gee, J.C., Gerig, G., 2006. User-guided 3D active contour segmentation of anatomical structures: Significantly improved efficiency and reliability. NeuroImage 31 (3), 1116–1128. doi:10.1016/j.neuroimage.2006.01.015.

Zang, Y.-F., Yong, H., Chao-Zhe, Z., Qing-Jiu, C., Man-Qiu, S., Meng, L., Li-Xia, T., Tian-Zi, J., Yu-Feng, W., 2007. Altered baseline brain activity in children with ADHD revealed by resting-state functional MRI. Brain Dev. 29 (2), 83–91. doi:10.1016/j.braindev.2006.07.002.

Zeeuw, C.I.D., Hoogenraad, C.C., Koekkoek, S.K.E., Ruigrok, T.J.H., Galjart, N., Simpson, J.I., 1998. Microcircuitry and function of the inferior olive. Trends Neurosci. 21 (9), 391–400. doi:10.1016/s0166-2236(98)01310-1.

Zeeuw, C.I.D., Lisberger, S.G., Raymond, J.L., 2020. Diversity and dynamism in the cerebellum. Nat. Neurosci. 1–8. doi:10.1038/s41593-020-00754-9.

Zhang, Y., Vakhtin, A.A., Jennings, J.S., Massaband, P., Wintermark, M., Craig, P.L., Ashford, J.W., Clark, J.D., Furst, A.J., 2020. Diffusion tensor tractography of brainstem fibers and its application in pain. PLOS ONE 15 (2), e0213952. doi:10.1371/journal.pone.0213952.